LIQUID PHASE METHANATION/SHIFT, MARSHALL E. FRANK, Chem Systems Inc., 747 Third Ave. New York, N.Y. 10017 - David B. Blum, Chem Systems Inc.-Research Center, 275 Hudson Street, Hackensack N.J.

Chem Systems' Liquid Phase Methanation/Shift (LPM/S) process economically converts high concentration CO synthesis gas to high Btu Gas. A development program with ERDA/AGA sponsorship has been under way since 1973. Recently the process concept has been extended to handle synthesis gas feeds wherein the hydrogen to carbon monoxide molar ratio is less than 3/1. In the liquid phase system, the methanation reaction and the water-gas shift reaction proceed simultaneously. The hydrogen produced by the shift reaction is utilized immediately for the methanation reaction. With synthesis gas feeds containing less than a 2/1 hydrogen to carbon monoxide ratio, a small amount of additional water (usually in the form of steam) must be added to the system to provide the necessary hydrogen for bulk CO conversion. The effluent gas from the liquid phase reactor is sent to a small, fixed bed, polishing reactor for complete conversion of the carbon monoxide. This paper describes recent experimental work in a bench scale unit and in a larger process development unit (PDU). Results have been correllated using an empirically derived kinetic model. The effect of water addition rate on carbon monoxide conversion and effluent gas composition has been determined for synthesis gas feeds with H_2/CO ratios ranging from 1/1 to 2/1. Life tests have been performed on catalysts under various polishing reactor conditions. Based on the bench scale and PDU results, the economics of the liquid phase methanation/shift process as it would be applied in a commercial size coal gasification plant have been determined.

Pilot Plant Operation of a Nonadiabatic Methanation Reactor

R. R. Schehl, H. W. Pennline, J. P. Strakey and W. P. Haynes

Energy Research and Development Administration
Pittsburgh Energy Research Center
4800 Forbes Avenue
Pittsburgh, PA 15213

INTRODUCTION

The development of efficient catalytic methanation reactors is essential to the commercialization of plants for converting coal to substitute natural gas. One of the most important problems facing researchers in this area is that of effective removal of the heat of reaction from the catalyst bed. The Energy Research and Development Administration, Pittsburgh Energy Research Center, is conducting bench-scale and pilot-plant scale studies of a variety of types of catalytic methanation reactors. Some of the earlier investigations (1, 2) included fixed-bed and fluidized-bed experiments using an assortment of supported catalysts and promoters. Later studies (3, 4, 5, 6) concentrated on Raney nickel catalyst thermally deposited onto stainless steel substrates and operated in reactors of varying geometrical configurations and differing modes of operation.

Two distinctly different types of methanation reactors utilizing thermally sprayed Raney nickel catalyst had heretofore been investigated; one, an isothermal reactor in which the Raney nickel was thermally sprayed onto either the internal or external surface of a tube with the heat of reaction being removed by circulating Dowtherm, the other, an adiabatic reactor with the catalyst bed consisting of parallel plate grid assemblies. The plates were constructed of stainless steel and coated on both sides with Raney nickel. The catalyst temperature in the adiabatic reactor is controlled by diluting the reactants in the feed stream to the reactor with recycled product gas. There are advantages and disadvantages to both reactor schemes and the present work is an effort to encorporate desirable features of each methanation scheme into a more efficient reactor system.

The hybrid reactor, as we have christened it, employs a Dowtherm jacket to remove an appreciable amount of the heat of reaction, while at the same time, some product gas is recycled through the reactor to control the reaction rate. The catalyst bed is in the form of an x-shaped stainless steel insert, thermally sprayed with Raney nickel. This insert may be easily replaced when the catalyst becomes deactivated.

REACTOR DESCRIPTION

The hybrid reactor experiments, HYB-17, 18, 19 and 20, were performed in a pilot plant scale reactor constructed of type 304 stainless steel 2 inch schedule 40 pipe. Surrounding the two inch reactor tube was a four inch diameter pipe jacket containing boiling Dowtherm in the annular space to remove a portion of the heat of reaction. The Dowtherm cooling system is depicted in figure 1. The temperature of the coolant is regulated by controlling the pressure in the cooling system. Nucleate boiling is assumed to take place on the outer surface of the reactor tube thereby providing a natural convective circulation of the Dowtherm. Dowtherm vapor is condensed via cooling water and returned to the reservoir.

The catalyst bed consisted of an x-shaped insert coated with Raney nickel catalyst. The cross member insert was two stainless steel 1 x 1 x 1/8 inch angles welded together, 14 ft long. The catalytic surface of the insert was prepared by sand-blasting the stainless steel surface with an iron-free grit and then depositing a

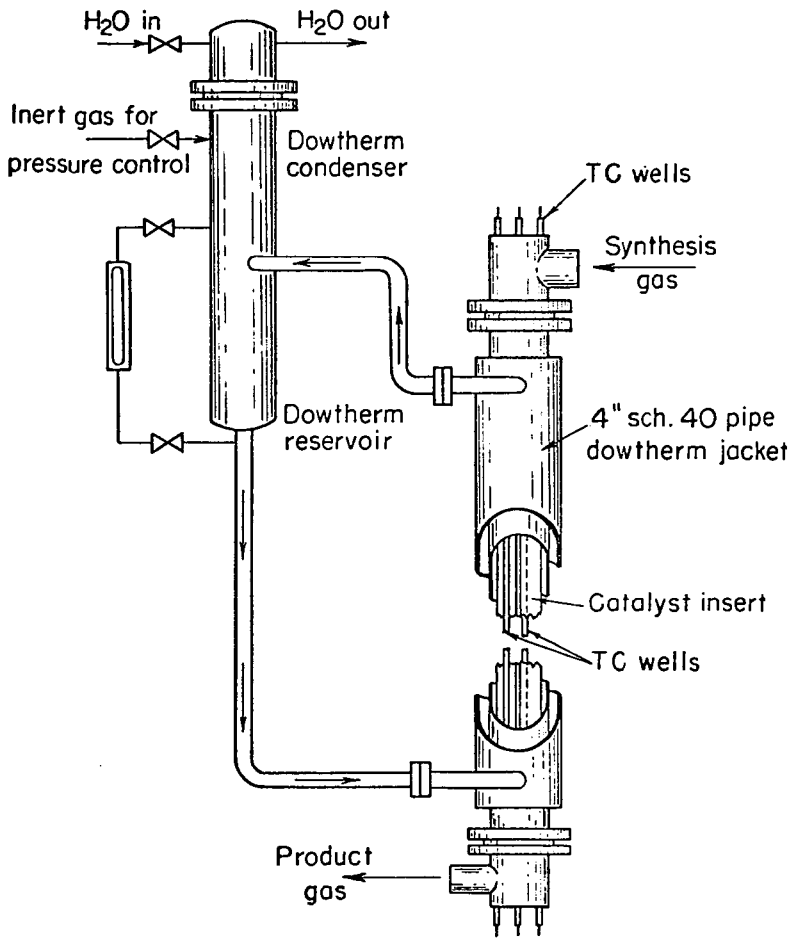

Figure 1. - Hybrid methanation reactor with Dowtherm cooling system.

light coat of bonding material consisting of 80% Ni and 20% Al to a thickness of about .007 inches. Subsequent to the bond coat, Raney nickel alloy powder (80-200 mesh) was thermally deposited onto the bond surface until the desired thickness was achieved (.023 inches). Two different methods were employed for the thermal deposition of Raney nickel onto the substrate. In runs 17 and 18 the catalyst was flame sprayed onto the surface with an oxy-hydrogen flame. A plasma arc with nitrogen as the carrier gas was used to deposit the catalyst for runs 19 and 20. Prior bench-scale studies indicated that plasma sprayed catalyst exhibited longer stability, hence, the method of catalyst deposition was one of the more important parameters studied in this sequence of runs.

The catalyst insert was placed in the reactor and then activated by passing a 2 wt. percent solution of NaOH through the reactor until approximately 70 percent of the aluminum in the Raney alloy was reacted. The extent of reaction was determined by measuring the quantity of hydrogen which evolves according to 3 moles of H_2 for every 2 moles of Al reacted. After activation, the catalyst was washed with distilled water until the pH of the effluent water was within one or two tenths that of the distilled water. The reactor was maintained under hydrogen until the temperature and pressure of the system was brought to synthesis conditions. Synthesis feed gas was then introduced gradually to the system to initiate the run.

Figure 2 illustrates a simplified flowsheet of the hybrid methanation pilot plant. Synthesis gas consisting of approximately 3 parts hydrogen and one part carbon monoxide is blended with recycled product gas. Product water vapor is condensed from the recycle stream before the recycle is mixed with the fresh feed gas. The ratio of recycled gas to fresh gas was from 5 to 8, depending upon the exposure velocity, for a fresh catalyst bed. The recycle ratio required to maintain some preselected maximum catalyst temperature then tended to increase as the catalyst activity declined with age. The mixed gas stream was preheated to the desired temperature before being introduced to the reactor. This temperature was generally the same temperature as that of the Dowtherm coolant.

A second stage clean-up methanator, not shown in figure 2, was used only during the latter periods of the runs when conversion in the primary reactor was declining. The clean-up reactor, an adiabatic reactor charged with a supported commercial nickel catalyst, was utilized to upgrade the quality of the product gas from the primary reactor.

OPERATING PROCEDURES AND RESULTS

The system pressure for all four hybrid reactor runs was 300 psig. The Dowtherm temperature in the cooling jacket as well as the inlet gas temperature was maintained at 300° C throughout all of the runs except for the last few hundred hours of Run 20, when these temperatures were raised to 325° C. Similarly, the maximum catalyst temperature was held at 400° C by adjusting the rate of recycled product gas. The maximum catalyst temperature was allowed to increase to 425° C during the latter portion of Run 20.

Catalyst temperature and gas temperature were measured at 3 inch intervals throughout the reactor on a daily basis. This was accomplished through the use of movable thermocouples in thermowells positioned as shown in figure 3. The thermocouple measuring the gas stream temperature was positioned in the geometrical center of one of the quandrants defined by the x-shaped insert and held in place by ceramic spacers. The thermowell designed to measure the catalyst temperature was first fastened into the "vee" formed by two fins. The bond and catalyst coatings were then sprayed over the thermowell at the same time that the fins were coated. A configuration of this type, with the catalyst essentially surrounding the thermowell,

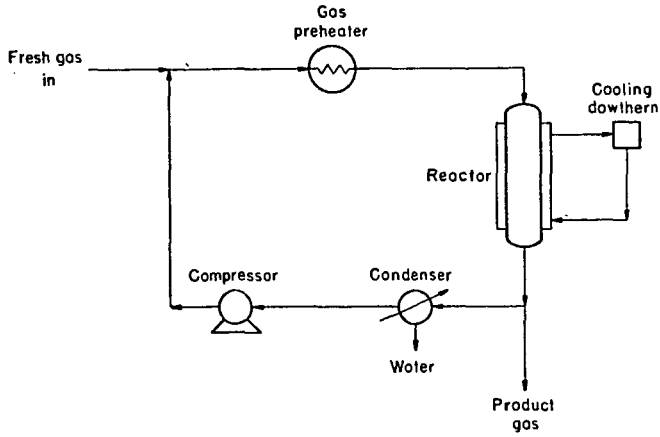

Figure 2. - Flow scheme of HYBRID reactor system.

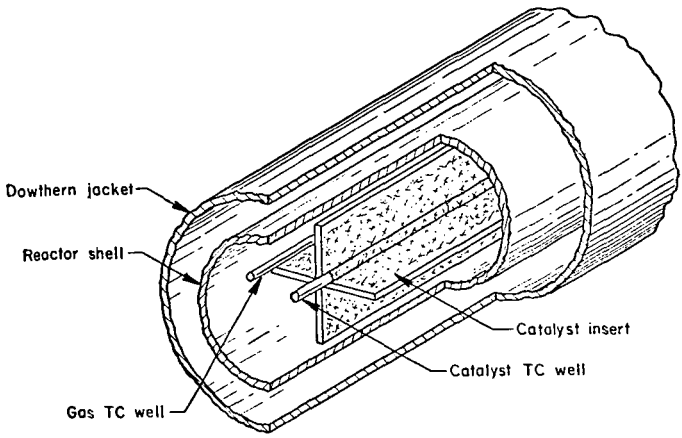

Figure 3. - View of catalyst insert and thermocouple wells.

should yield an excellent measurement of maximum temperature that the catalyst experiences. The gas stream composition was also measured as a function of distance through the catalyst bed. Gas samples were taken every one-eighth of the reactor length with a movable probe which was guided by a slit tube. The gas composition profile was measured only when operating conditions were changed rather than on a daily basis.

Run HYB-17: Seven two ft. inserts coated with flame sprayed Raney nickel were used in Run HYB-17. The reactor was operated at exposure velocities of 20, 30, and 40 scfh/ft^2. Exposure velocity is calculated as the ratio of scfh of synthesis gas (3 parts H_2 to 1 part CO) to the superficial catalyst surface area. An exposure velocity of 30 scfh/ft^2 corresponds to a space velocity of 806 hr^{-1}. Once again, the space velocity is based on a 25 percent CO fresh feed gas flow rate. This first hybrid reactor experiment lasted only 671 hours. The run was terminated when CO conversion decreased to 96.6 and the concentration of CO in the product gas reached 3 percent. Overall performance of this catalyst bed was not outstanding with a production of only 15.0 mscf of CH_4 per pound of catalyst (before leaching). Operating parameters and product gas characteristics are presented in figure 4. Catalyst bed data for Run HYB-17 as well as the three successive runs are listed in Table 1.

Table 1. - Catalyst Bed Data

	HYB-17	HYB-18	HYB-19	HYB-20	HYB-21
Catalyst Type	Flame-Sprayed Raney		Plasma Sprayed Raney		Cast Raney
Wt Pct Nickel	42[a]	42[a]	42[a]	42[a]	42[a]
Pct Activated	71.4[b]	70.6[b]	70.1[b]	70.0[b]	100.0[c]
Reactor Diameter X Length, in.	2 x 168	2 x 168	2 x 168	2 x 168	2 x 170
Reactor Volume, ft^3	0.326	0.326	0.326	0.326	0.330
Weight of Unactivated Catalyst, lb	2.78	2.24	2.43	1.70	10.64
Superficial Area of Catalyst, ft^2	8.75	8.75	7.58	8.46	11.20
Fin Thickness, in.	0.124	0.122	0.125	0.129	0.150
Avg. Bond Coat Thickness, in.	0.008	0.007	0.007	0.006	—
Avg. Catalyst Thickness, in.	0.03	0.023	0.023	0.013	0.050

[a] before leaching

[b] theoretical (based on H_2 evolution)

[c] 100% theoretical leaching of 0.05 inches

Run HYB-18: Flame sprayed Raney nickel was again used in Run HYB-18. Operating conditions were comparable to those of HYB-17 with the exception that the catalyst was exposed to a higher space velocity (1344 hr^{-1}, 50 scfh/ft^2) during a large portion of the run. This experiment lasted almost 3 times longer than the previous run. The run was voluntarily terminated after 2073 hours on stream when the CO conversion reached 95.6 percent and the CO concentration in the product gas was nearly 4 percent. It should be noted in figure 5 that decreasing the Dowtherm temperature from 300° C to 275° C at about 1950 hours on stream was responsible for a large decrease in conversion. CO conversion just prior to this time was

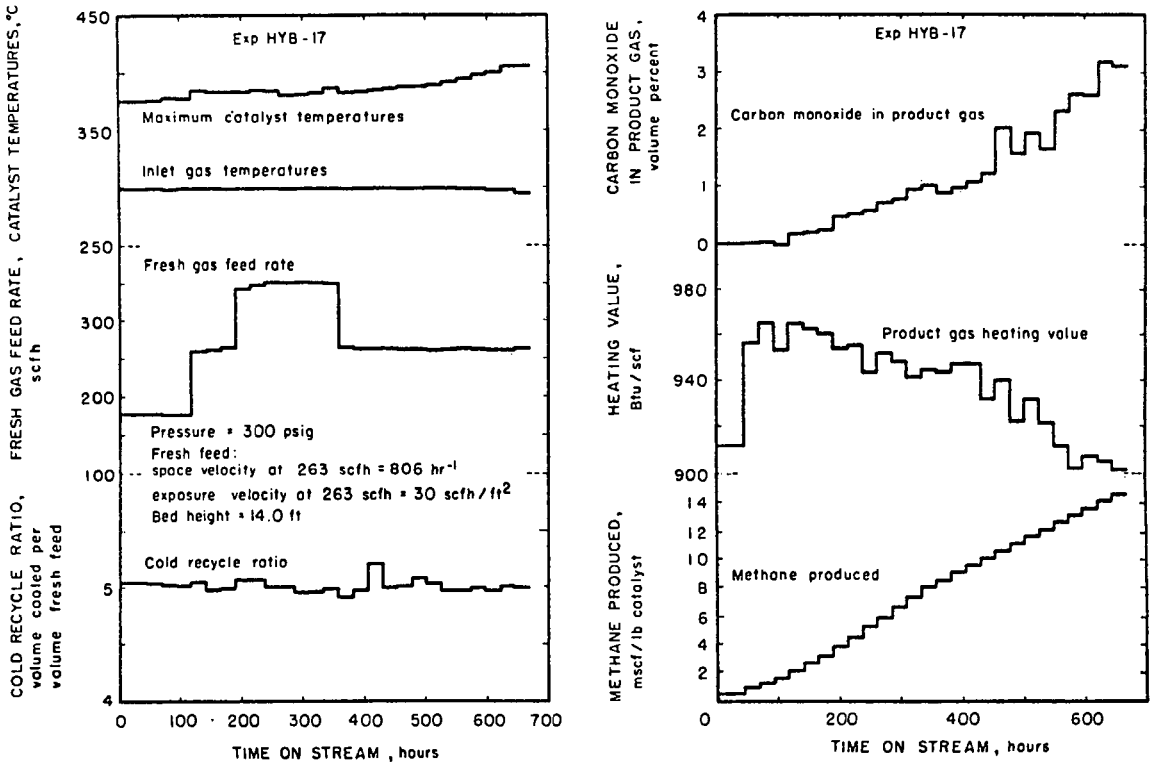

Figure 4. - Reactor conditions and product gas characteristics for Run HYB-17.

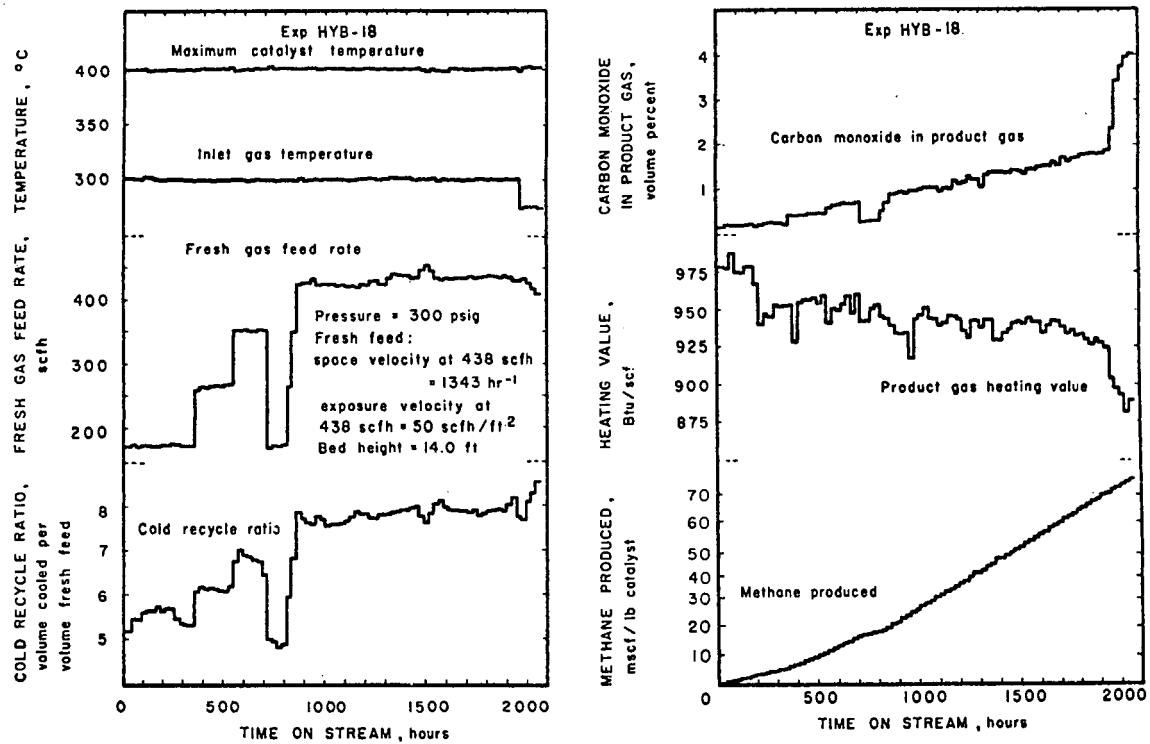

Figure 5. - Reactor conditions and product gas characteristics for Run HYB-18.

still rather acceptable at 98 percent. Due to greater catalyst stability, methane production was much higher for Run HYB-18 with a total of 75.2 mscf per pound of catalyst. Data pertinent to Run HYB-18 are illustrated in figure 5.

Typical stream flowrates and compositions are listed in table 2 for experiment HYB-18. These are data averaged over a 24 hour period and representative of the operating conditions during each of the exposure velocities investigated (20, 30, 40 and 50 scfh/ft^2). The last period represents the reactor operation with a Dowtherm temperature of 275° C. It should be noted that, at this temperature, CO conversion decreased significantly, and as a direct result, the heating value of the product gas decreased to 898.1 Btu/scf.

Run HYB-19: Recent experiments performed on bench-scale methanation reactors using plasma sprayed Raney nickel catalyst indicated that catalyst coatings prepared in this manner demonstrated a longer life. In an effort to test these findings in a larger scale reactor, an x-shaped substrate, identical to that used in runs HYB-17 and HYB-18 was plasma sprayed with catalyst and operated under conditions similar to those used in the previous two runs. Deactivation of the catalyst was rather rapid, with the experiment lasting only 1100 hours. Final CO conversion declined to 97.3 percent with 2.35 percent CO in the product gas. Methane production for this run was 36.6 mscf per pound of catalyst. Operating conditions for this run are shown in figure 6. One plausible explanation for the relatively poor performance of the catalyst in this experiment might lie in the leaching procedure. The activation time required for 70% aluminum leaching was much shorter, 4.6 hours compared to 18 hours in Run HYB-18. It was discovered that the NaOH solution was inadequately mixed resulting in an initial caustic concentration higher than the usual 2 percent.

Run HYB-20: This experiment was, essentially, a duplication of Run HYB-19. Operating parameters and product gas characteristics are given in figure 7. Methane production for this plasma sprayed catalyst was significantly better than HYB-19 with a total of 75 mscf per pound of catalyst. Final CO conversion stood at 97 percent with 2.55 percent CO in the product gas. The reactor was on stream for a total of 2081 hours. As indicated in figure 7, the Dowtherm temperature was increased to 325° C during the last portion of this run. Correspondingly, the maximum catalyst temperature was allowed to increase to 425° C. The increase in catalyst temperature was accompanied by a decrease in the quantity of recycled product gas required. Contrary to what might be expected, however, an increase in catalyst temperature did not significantly improve CO conversion. The conversion remained about the same, at 97.7 percent.

HYB-21: A fifth hybrid test has just been initiated. Preliminary results of this run are given in figure 8. The catalyst bed in this run differs from the previous four in that cast Raney nickel inserts were used rather than a thermally spray coated stainless steel insert. The castings were made of 42-58 percent Ni-Al alloy; each being six inches long and having 8 fins. The castings were formed with a hole along the axis to accomodate a thermocouple well to measure catalyst temperature. The catalyst surface was activated to a depth of .05 inches and operated under conditions similar to those for Run HYB-20. The data shown in figure 8 for the first 384 hours on stream indicate greater initial CO conversion and no detectable catalyst deactivation.

At the termination of each run, samples of spent Raney nickel catalyst were removed from the catalyst insert and subjected to wet chemical analysis, x-ray diffraction, BET surface and pore size distribution analysis. Two catalysts, one flame sprayed Raney nickel and one plasma sprayed Raney nickel, were measured for nickel surface area. Table 3 summarizes the results from chemical analysis and x-ray diffraction of the samples taken from the four runs. An appreciable carbon

Table 2. - Experiment HYB-18, Selected Test Data

Time on Stream.....hr	335	527	695	1640	2000
Temperatures					
Dowtherm.....°C	300	300.	300.	300.	275.
Gas Inlet.....°C	300.	300.	300.	300.	276.
Maximum Catalyst.....°C	400.	400.	400.	400.	401.
Pressure.....psig	300.	300.	300.	300.	300.
Feed Gas					
Rate.....scfh	175.	269.5	354.1	433.6	433.7
H_2.....vol pct.	75.5	76.1	74.6	75.9	75.9
CO..... "	23.8	3.0	23.6	23.7	23.4
CO_2..... "	.3	.3	.1	.2	.2
N_2..... "	.2	.4	1.5	.1	.4
CH_4..... "	.2	.2	.2	.1	.1
H_2O..... "	.0	.0	.0	.0	.0
Exposure Velocity.....scfh/ft^2	20.	30.8	40.5	49.6	49.6
Space Velocity.....hr^{-1}	673.	1036.5	1361.9	1667.7	1668.1
Mixed Feed Gas					
Rate.....scfh	1112.2	1912.4	2748.4	3870.1	3779.1
H_2.....vol pct	17.9	16.0	16.1	14.5	19.4
CO..... "	3.9	3.7	3.7	4.0	5.1
CO_2..... "	0.2	.2	.2	.7	.5
N_2..... "	0.7	.8	.7	1.2	.3
CH_4..... "	77.2	79.2	79.2	79.5	74.0
H_2O..... "	.1	.1	.1	.1	.1
Inlet Velocity.....ft/sec	1.4	2.5	3.6	5.0	4.7
Inlet Reynold's No..... "	3357.	5885.	8465.	12042.	11548.
Exposure Velocity.....scfh/ft^2	127.1	218.6	314.1	442.3	431.9
Space Velocity.....hr^{-1}	4278.	7355.	10571.	14885.	14535.
Volume Recycle/Volume Fresh Gas	5.4	6.1	6.8	7.9	7.7
Product Gas					
Rate..... scfh	40.9	64.4	88.4	105.9	112.1
H_2.....vol pct	6.8	6.0	7.2	6.6	11.6
CO..... "	.2	.5	.7	1.5	3.3
CO_2..... "	.1	.2	.2	.7	.6
N_2..... "	.8	.9	.6	1.2	.3
CH_4..... "	87.9	89.2	87.9	87.1	81.3
H_2O..... "	4.2	3.2	3.4	2.9	2.9
Conversion					
CO..... pct	99.7	99.5	99.2	98.4	96.2
H_2..... pct	97.7	98.0	97.4	97.8	95.9
Heating Value.....Btu/scf	953.7	955.6	948.4	935.1	898.1
Carbon Recovery..... pct	91.6	98.3	98.8	93.5	95.6
Hydrogen Recovery..... pct	92.2	89.1	97.2	90.0	90.7
Oxygen Recovery..... pct	98.9	89.1	103.3	99.1	100.4

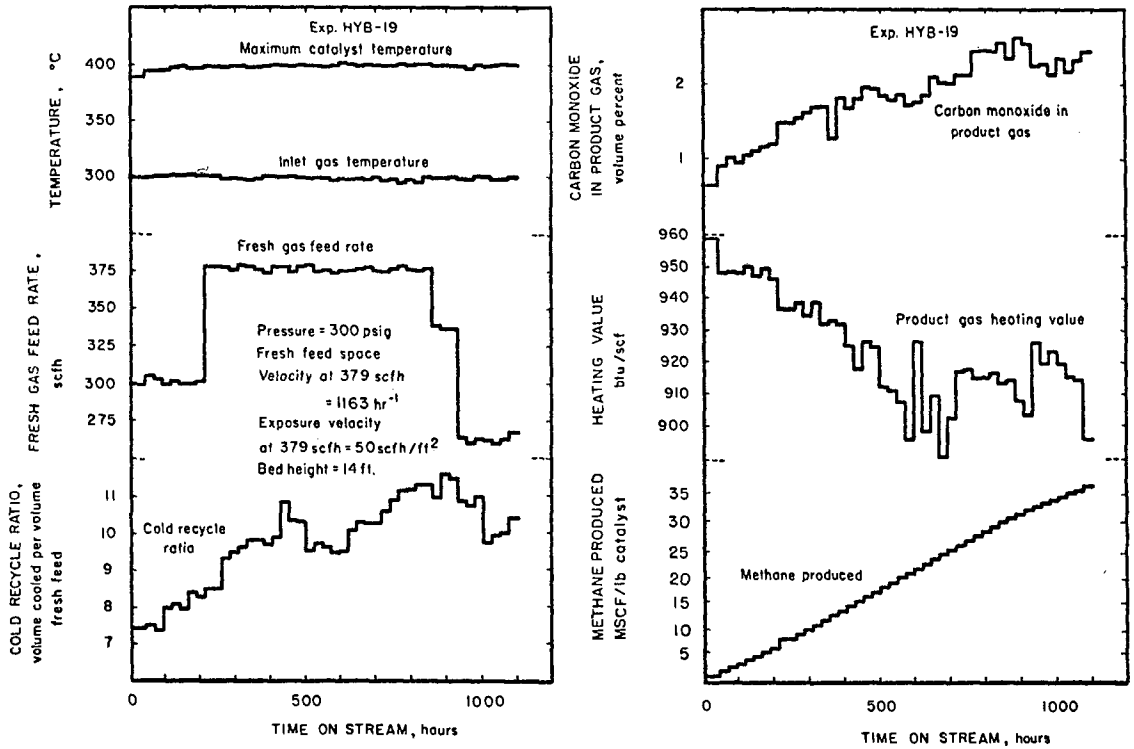

Figure 6. - Reactor conditions and product gas characteristics for Run HYB-19.

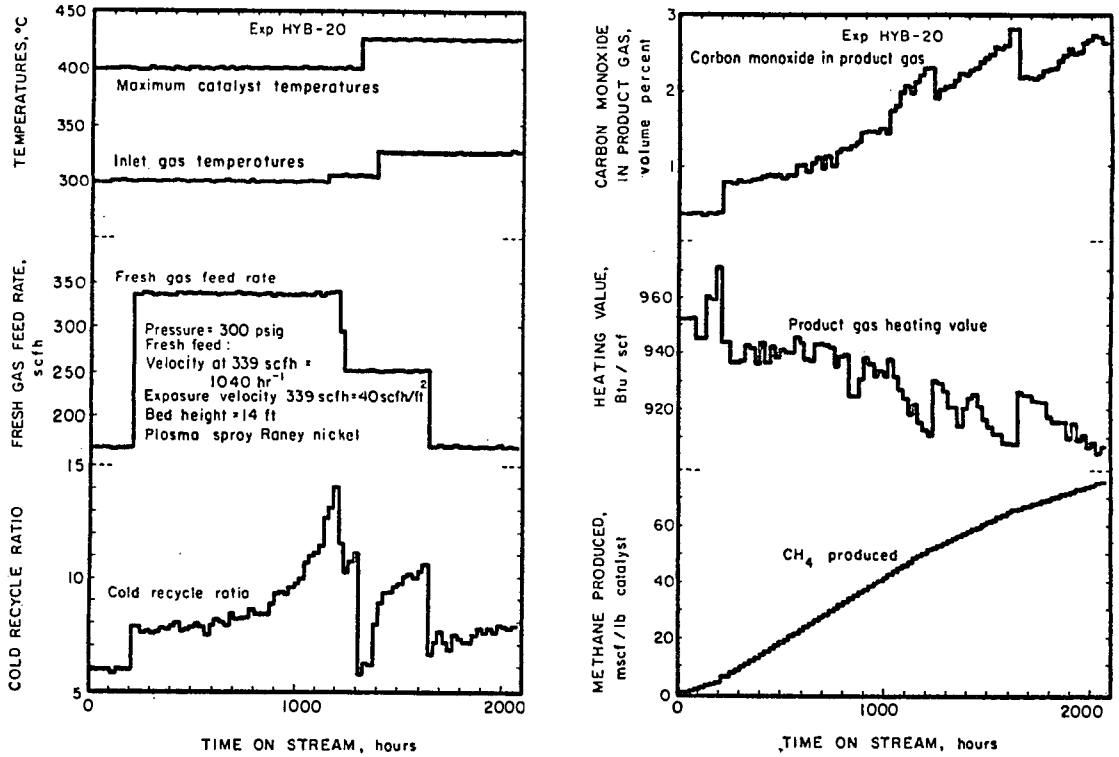

Figure 7. - Reactor conditions and product gas characteristics for Run HYB-20.

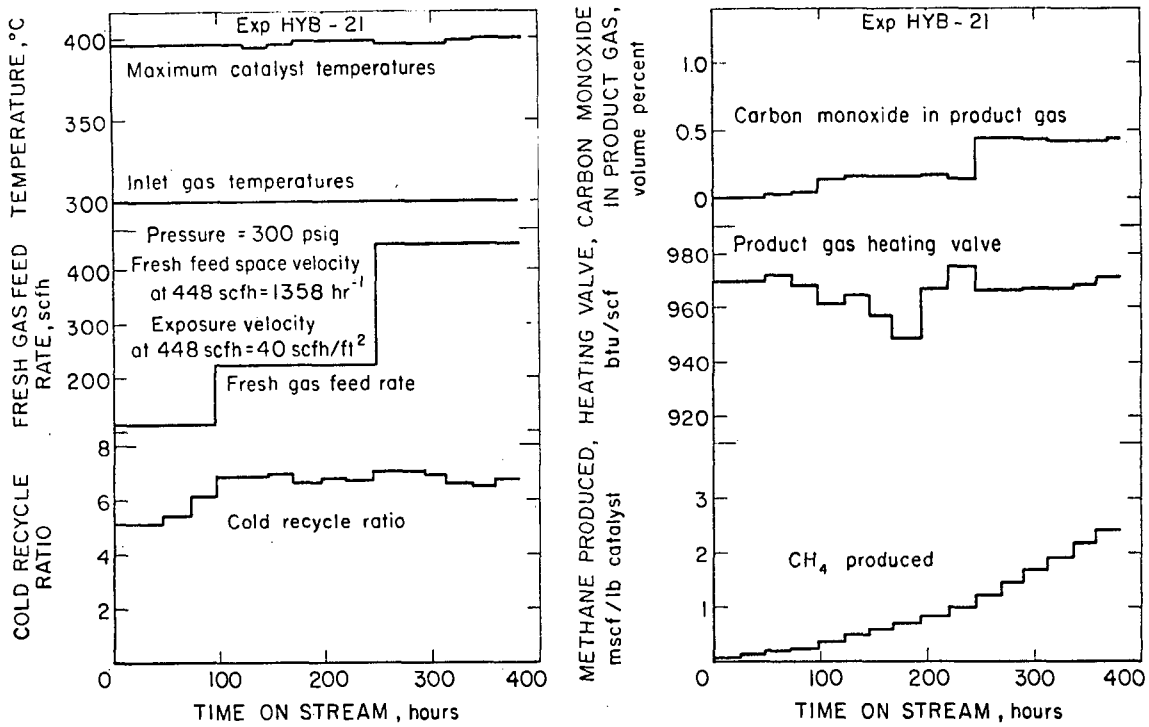

Figure 8. - Reactor condition and product gas characteristics for Run HYB-21.

Table 3. - Analysis of Spent Catalysts

	Ni	Al	C	S	Fe	Na	Species
HYB-17							
Inlet	68.1	8.6	4.68	-	0.27	0.08	Ni_3C
Center	74.6	8.8	1.71	-	0.24	0.08	Ni_3C, Ni
Outlet	72.3	9.0	0.20	-	0.25	0.08	Ni
HYB-18							
Inlet	64.1	10.4	2.0	0.3	0.5	4.5	Ni_3C
Center	68.0	11.7	0.7	0.2	0.4	4.9	-
Outlet	69.0	11.6	0.5	0.3	0.7	6.5	Ni
HYB-19							
Inlet	75.7	8.6	3.0	0.2	0.5	0.08	Ni, Ni_3C
Center	77.1	7.3	1.6	0.3	0.5	0.03	Ni
Outlet	75.7	6.6	1.1	0.2	0.4	0.03	Ni
HYB-20							
Inlet	76.5	8.8	3.4	0.1	0.3	<0.01	Ni_3C
Center	80.3	8.3	1.0	0.4	0.4	<0.01	Ni
Outlet	79.4	8.4	0.3	2.2	0.4	<0.01	Ni

profile along with nickel carbide is found in every case. Other contaminants such as S, Fe, and Na are not present in amounts significantly greater than those found in unactivated catalyst except for high sodium concentrations on Run HYB-18 catalyst. This probably is indicative of insufficient rinsing of the catalyst subsequent to the activation step. The high sulfur concentration measured at the exit of HYB-20 is unexplained. Possibly sampling and/or analysis errors are involved. Analysis of this sample is being repeated. Iron contamination had been a problem in experiments prior to the hybrid reactor tests. Iron carbonyl can form by reaction of CO at high pressure and low temperature (100° - 200° C) with carbon steel piping. The carbonyl is carried into the hot reactor where it thermally decomposes according to the reaction:

$$2Fe\ (CO)_5 \rightarrow 5C + 2Fe + 5CO_2$$

and deposits on the nickel catalyst creating an iron catalyst. At methanation temperatures, carbon deposition occurs on the iron and further fouls the catalyst. Iron concentrations as high as 22 percent in the catalyst at the reactor inlet had been detected in previous runs. This was accompanied by high carbon content. Before initiating the hybrid reactor experiments, all carbon steel piping in the pilot plant was replaced with stainless steel. Examination of the iron concentrations found on the spent catalyst samples from the hybrid runs in table 3 indicates that this was successful in alleviating the iron contamination problem. The BET surface areas, pore volumes and pore radii are shown in table 4. Measured BET surface area for HYB-17 and HYB-20 appear to be somewhat smaller than those for the other runs. No other trends in the data were clearly evident. Also shown on table 4 are the nickel metal surface area measurements as determined by hydrogen chemisorption. Metal surface area measurements were performed on a flame-sprayed catalyst, Run HYB-18, and a plasma sprayed catalyst, Run HYB-20. In both instances, metal surface area is lower at the reactor exit than at the inlet while in general, being lower for HYB-20 than for HYB-18. There is no immediate explanation for these trends in the data. Nickel metal surface area for freshly activated catalyst is in the neighborhood of 12 m^2/gm. The tentative conclusion regarding the cause for catalyst deactivation for this series of experiments, in view of the limited amount of data available, is the formation of nickel carbide and possibly additional carbon formation on the catalyst surface. It was not possible to distinguish free carbon from carbidic carbon.

Table 4. - Surface Areas Of Spent Catalysts

	Surface Area m^2/gm	Pore Volume cm^3/gm	Avg. Pore Radius Å	Nickel Surface Area m^2/gm
HYB-17				
Inlet	30.5	.076	50.07	
Outlet	23.7	.055	46.07	
HYB-18				
Inlet	53.4	.053	45.05	6.0
Outlet	50.2	.060	53.51	4.5
HYB-19				
Inlet	44.3	.095	42.8	
Outlet	32.8	.11	66.7	
HYB-20				
Inlet	32.77	.067	40.6	2.5
Outlet	23.73	.078	65.7	<1.0

MATHEMATICAL MODELING

Several recent publications (7, 8, 9, 10, 11) have discussed a one-dimensional mathematical model along with several applications of the model to tube-wall and parallel-plate, adiabatic (hot-gas-recycle) methanation reactors. Incorporated in the model was a postulated poisoning mechanism which obeyed an irreversible Langmuir-Hinschelwood type of rate equation. This one-dimensional model has been appropriately modified to describe the chemical and physical processes occurring in the hybrid methanation reactor.

The kinetic rate expression for the conversion of carbon monoxide to methane according to the reaction

$$CO + 3H_2 \rightarrow CH_4 + H_2O,$$

is taken to be that proposed by A. L. Lee (12, 13) which provides a reasonable fit to data reported by IGT. Lee's rate expression, developed from data for supported commercial nickel catalysts is of the form,

$$-r_{CO} = \frac{A\, e^{(-E/RT_C)}\, \tilde{C}_{CO}\, \tilde{C}_{H_2}^{\,1/2}}{1 + k_1 \tilde{C}_{H_2} + k_2 C_{CH_4}} \qquad 1)$$

Since the catalyst is deposited in a very thin layer, the catalyst thickness is neglected in the model and is considered to be only an active superficial surface. The kinetic rate is expressed as the number of moles of CO converted per unit time per unit superficial surface area of catalyst. The symbols, $\tilde{C}$, signify that these are concentrations at the surface of the catalyst as opposed to concentrations in the bulk stream. It should be noted that the concentration of methane at the catalyst surface is assumed to be the same as the bulk methane concentration. Due to the relatively large quantity of product gas that is recycled through the catalyst bed, methane is the major constituent in the gas at every point in the reactor. The assumption is made that negligible error is introduced by ignoring the methane concentration gradient between the bulk gas and the catalyst surface.

The construct envisioned for the description of the processes occurring in the hybrid reactor is the following. The reacting gas, flowing through a conduit in turbulent flow, is considered to be thoroughly mixed in the radial direction, i.e., there are no thermal or concentration gradients across the turbulent core (see figure 9). The reactants (CO and H_2) are transported across the laminar sublayer, adsorbed, react to form methane and water, and the products diffuse back into the turbulent core. There will be thermal and concentration gradients across the laminar film, the magnitudes of which depend upon the extent of diffusion control. Energy released in the methanation reaction is removed from the catalyst by convective heat transfer to the cooler bulk gas and thence to the cooling jacket and by radiation from the catalyst to the cooling jacket. A portion of the heat of reaction is also removed as sensible heat to the gas.

At steady state conditions there is no net change in reactant concentrations at the catalyst surface, thus, the rate of reaction must equal the rate at which CO and H_2 diffuse to the surface. The mass transfer rates are given by,

$$-r_{CO} = k_C\,(C_{CO} - \tilde{C}_{CO}) = j_{CO} \qquad \text{2-a)}$$

$$-r_{H_2} = -3r_{CO} = k'_C\,(C_{H_2} - \tilde{C}_{H_2}) = j_{H_2} \qquad \text{2-b)}$$

where k_C and k'_C are the film mass transfer coefficients for CO and H_2 respectively. The mass transfer coefficients are calculated, for a given Reynold's number, from the standard j-factor correlation (14, 15).

The following equations are taken to describe the heat transfer in the system.

$q = r_{CO}\mathcal{H}$ rate of heat generated by reaction 3-a)

$q_1 = h(T_C - T_G)$ heat flux between catalyst and turbulent core 3-b)

$q_2 = k\varepsilon\,(T_C^{\,4} - T_W^{\,4})$ radiation heat flux between catalyst and cooling jacket 3-c)

$q_3 = h'\,(T_C - T_W)$ heat flux by conduction through direct contact of insert with cooling wall 3-d)

$q_4 = h\,(T_G - T_W)$ heat flux between turbulent core and cooling wall 3-e)

$C_P M \dfrac{\partial T_G}{\partial a}\,\delta a = q_1\delta a - q_4\delta a'$ rate change of sensible heat of the gas 3-f)

In addition, we have the equation for the conservation of energy,

$$q = q_1 + q_2 + q_3. \qquad \text{3-g)}$$

In order to calculate the global rate of reaction at any point in the reactor, equations 1), 2), and 3) must be solved simultaneously. The method of finite differences is utilized to calculate local bulk concentrations and temperatures throughout the length of the reactor. The model used to describe catalyst deactivation in previous experiments has been reported elsewhere (7, 8) and will not be reiterated. This deactivation mechanism was found to inadequately predict deactivation rates for the hybrid methanation reactor. It is possible that, due to system plumbing

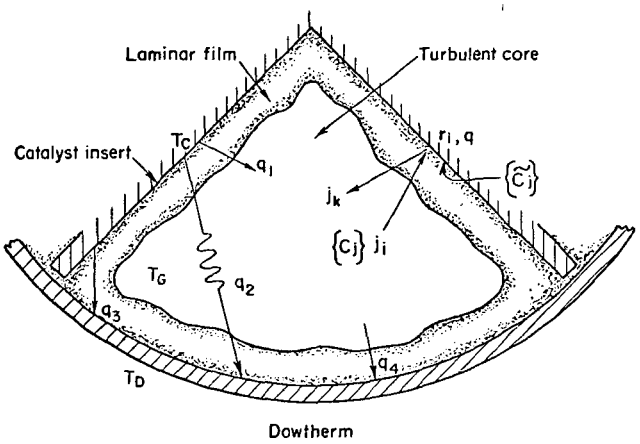

Figure 9. - Cross-section view of a quadrant of the reactor.

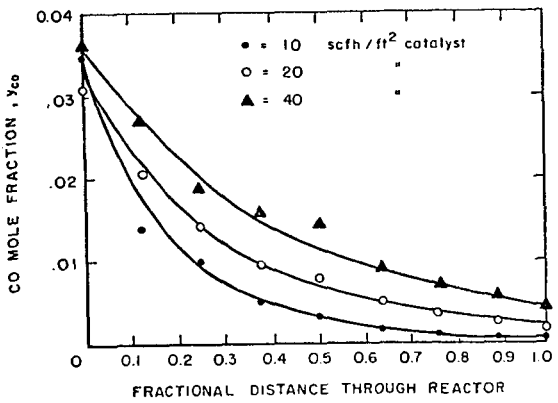

Figure 10. - Carbon monoxide mole fraction profiles for Run HYB-21. Solid lines indicate model predictions.

modifications, i.e. the substitution of carbon steel with stainless steel pipes, catalyst activation procedures, or the intrinsic difference in mode of reactor operation, the principal agent responsible for catalyst deactivation differs between the hybrid reactor and reactors previously operated. Nevertheless, the model is capable of satisfactorily predicting initial reactor performance. As an example, figures 10 and 11 illustrate the fit of the model to experimental composition and temperature profile data from Run HYB-21. Figure 10 is a plot of CO mole fraction as a function of distance through the reactor. Gas stream compositions were measured at 21 inch intervals through the reactor. The data represente operation at exposure velocities of 10, 20 and 40 scfh/ft^2 catalyst and wer taken early in the run before any deactivation of the catalyst was evident. The points indicate experimentally measured values whereas the solid lines represent the profiles calculated from the model. Agreement between model and experiment is seen to be quite good.

Temperature profiles for both catalyst and gas phase are illustrated in Figure 11. The three plots, once again, represent operation at 10, 20 and 40 scfh/ft^2 catalyst. The open circles are measured catalyst temperature while the ▲'s are gas phase temperatures. The temperatures predicted by the model (solid lines) are in good agreement with measured values. At the higher exposure velocities, the differences between model and measured values are, at most, 10-15° C. The percentages of the total heat liberated by the reaction which is transferred to the Dowtherm coolant are 86, 73 and 61% for the exposure velocities 10, 20, and 40 scfh/ft^2 catalyst, respectively.

SUMMARY

Four experiments were completed using the hybrid methanation reactor. A fifth experiment utilizing cast Raney nickel inserts has been initiated and preliminary results are encouraging. Each of the first four runs was terminated voluntarily with final CO conversions no less than 95-97 percent. The reactor was satisfactorily operated at an exposure velocity of 50 scfh/ft^2, comparable to those attainable in the tube-wall reactor, yet, as a result of the bed design, the catalyst can be easily replaced. The recycle ratio in a hot-gas-recycle methanator required to maintain a 100° C gas temperature difference across the catalyst bed is about 10/1. At comparable exposure velocities, the recycle ratio required to hold the catalyst temperature below 400° C in the hybrid reactor is as little as 5/1 - 6/1.

Although the hybrid reactor had a higher average productivity of methane per pound of catalyst than previous TWR and HGR experiments, it is possible that this is the result of decreasing the amount of iron carbonyl in the system rather than the nature of the reactor. Data, resulting from the four completed runs, do not indicate that plasma sprayed Raney nickel catalyst demonstrates a greater life at the pilot plant scale than flame sprayed Raney nickel. Data from the test using cast Raney nickel inserts are, of course, incomplete at the present time. Catalyst stability continues to be of prime concern in the research efforts at Pittsburgh Energy Research Center.

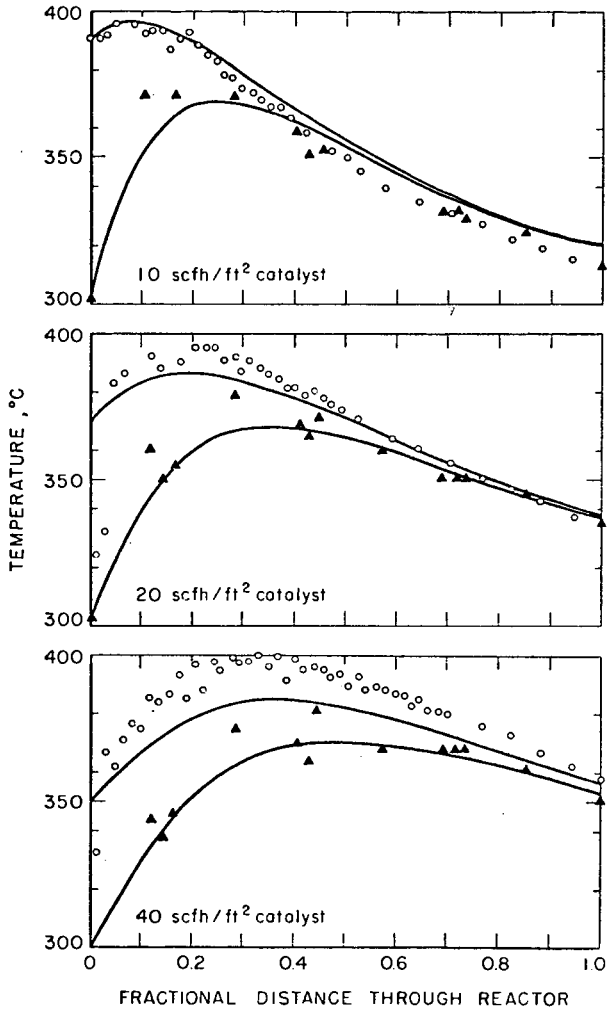

Figure 11. - Catalyst (O) and Gas (▲) temperature profiles for Run HYB-21. Solid lines indicate model predictions.

NOMENCLATURE

A= preexponential factor

C= concentration in bulk gas (lb mol/ft^3)

$\tilde{C}$= concentration at catalyst surface (lb mol./ft^3)

C_p= specific heat of gas (Btu/lb.mol. - °F)

E= activation energy (Btu/lb mol)

$\mathcal{H}$= heat of reaction (Btu/lb mol)

h= heat of transfer coefficient (Btu/hr-ft^2 - °F)

j= mass flux (lb. mol./hr-ft^2)

k= constant (Btu/hr-ft^2 - $°R^4$)

k_C= mass transfer coefficient (lb.mol./hr-ft^2-concentration difference)

k_1,k_2= equilibrium constant's

M= gas molar flowrate (lb.mol./hr)

q= rate of heat generated (Btu/hr-ft^2)

q_1= heat flux from catalyst to gas (Btu/hr-ft^2)

q_2= radiation heat flux between catalyst and cooling jacket (Btu/hr-ft^2)

q_3= heat flux by conduction through direct contact of insert with cooling wall (Btu/hr-ft^2)

q_4= heat flux from gas to cooling wall (Btu/hr-ft^2)

R= gas constant (Btu/lb.mol. - °R)

r= rate of reactant conversion (lb.mol./hr-ft^2 catalyst)

T= temperature (°R)

ε= emissivity (dimensionless)

δa= incremental catalyst surface area (ft^2)

δa'= incremental cooling wall surface area (ft^2)

REFERENCES

1. Grayson, M., Demeter, J.J., Schlesinger, M.D., Johnson, G.E., Jonakin, J., and Meyers, J.W., "Synthesis of Methane", BuMines RI-5137, July 1955, 32 pp.

2. Schlesinger, M.D., Demeter, J.J., Greyson, M., "Catalyst for Producing Methane From Hydrogen and Carbon Monoxide", Industrial and Engineering Chemistry, 48, pp. 68-70, 1956.

3. Forney, A. J., Demski, R. J., Bienstock, D., and J. H. Field, "Recent Catalyst Developments in the Hot-Gas-Recycle Process". BuMines RI-6609, 1965, 32 pp.

4. Demeter, J.J., Youngblood, A.J., Field, J.H., and Bienstock, D., "Synthesis of High-Btu Gas in a Raney Nickel Coated Tube-Wall Reactor", BuMines RI-7033, 1967, 17 pp.

5. Haynes, W.P., Elliott, J.J., and Forney, A.J. "Experience with Methanation in Catalysts", 163rd National Meeting of American Chemical Society, Boston, Mass. April 10-14, 1972, Vol. 16, No. 2 pp. 47-63.

6. Haynes, W.P., Forney, A.J., Elliott, J.J., Pennline, H.W., "Synthesis of Methane in Hot-Gas-Recycle Reactors Pilot Plant Tests", ACS Fuels Division Preprint, Sept., 8-13, 1974, Vol. 19, No. 3, pp 10-42.

7. Haynes, W.P., Schehl, R.R., Weber, J.K., and Forney A.J., "Pilot Plant Study of An Adiabatic Parallel Plate Methanation Reactor " Paper presented at the 68th annual meeting of the American Institute of Chemical Engineers, LosAngeles, Calif., Nov. 16-20, 1975.

8. Schehl, R.R., Haynes, W.P., and Forney, A.J., "Catalyst Deactivation in Hot-Gas-Recycle Methanation Reactors, A Mathematical Model," ERDA PERC/RI-75/3, 1975, 22 pp.

9. Schehl, R.R., Haynes, W.P., and Forney, A.J., "Calculating Catalyst Temperature in a Hot-Gas-Recycle Methanation Reactor", ERDA PERC/RI-75/1, 1975, 12 pp.

10. Ralston, T.D., Haynes, W.P., Forney, A.J. and Schehl, R.R., "Tube-Wall Methanation Reactors With Combined Diffusion and Kinetic Resistance", BuMines RI-7941, 1974, 15 pp.

11. Wei, V.T., and Chen, J., "Tube-Wall Methanation Scale-up for Bureau of Mines SYNTHANE Coal Gasification Process Prototype Plant", Presented at the Fourth Joint Chemical Engineering Conference, Vancouver, British Columbia, Canada, September 10, 1973.

12. Lee, A.L., "Methanation for Coal Gasification" Clean Fuel for Coal Symposium, Chicago, Illinois, September, 1973.

13. Lee, A.L., Feldkirchner, H.L. and Tajbl, D.J., "Methanation for Coal Hydrogasification" Symposium on Hydrogen Processing of Solid and Liquid Fuels, American Chemical Society, Chicago, Illinois, September 13-18, 1970, Vol. 14, No. 4, Part I, pp 126.

14. Treybal, R.E., Mass Transfer Operations McGraw-Hill Book., Co., Inc., New York, 1955, p. 55.

15. Welty, J.R., Wicks, C.E. and Wilson, R.E., Fundamentals of Momentum, Heat and Mass Transfer, John Wiley and Sons, Inc., New York, 1969, p. 580.

A HIGH-TEMPERATURE METHANATION CATALYST FOR SNG APPLICATIONS

COLIN WOODWARD

Imperial Chemical Industries Limited, Agricultural Division, Billingham, Cleveland, TS23 1LD, England.

INTRODUCTION

The political and economic background to the development of coal-based Substitute Natural Gas processes will be familiar to readers and, therefore, need not be detailed herein. The technical problem can be regarded very simply as having two parts, namely the gasification of coal followed by conversion of the product gas into SNG. Proven commercial processes, eg Koppers-Totzek, Lurgi, etc exist for coal gasification and several second generation processes are in various stages of development in the United States and elsewhere. The compositions of gases produced by these processes differ depending upon operating conditions ie pressure, temperature, steam addition, etc. In general, however, dry gas compositions are typically in the range:

CO_2	0 - 30%
CO	10 - 60%
H_2	25 - 75%
CH_4	0 - 20%

Alternative methods of upgrading such a gas to pipeline quality exist, the major problem being to combine the degree of, highly exothermic, methanation required with a low final exit temperature compatible with favourable thermodynamic equilibrium for methane formation. A process incorporating a high recycle ratio of product gas back through the methanator has been described (1) as a means of moderating the temperature rise in the methanator. A more elegant and economic solution, however, is a straight-through process using a series of methanators operating at successively lower exit temperatures (2,3). The viability of such a scheme depends upon the availability of a methanation catalyst, or catalysts, capable of operating under the design conditions for commercially acceptable periods. The purpose of the work described in this paper was to develop and demonstrate such a catalyst. This work comprised part of a collaborative agreement between ICI and Krupp-Koppers GmbH to develop processes for the production of SNG from coal based upon the Koppers-Totzek coal gasification process.

EXPERIMENTAL

Process Design

The basic philosophy during this programme was to take a "typical" gas composition, to subject it to the type of methanation process necessary to produce SNG and to evaluate the performance of various catalysts, commercially proven and experimental, in the duties involved. The gas composition selected appears in Table 1 (column 1) and will be seen to have $H_2 + CO = 74\%$ (dry basis). While not referring specifically to a particular gasification process, this is representative of the composition of gas to be methanated. In fact, the virtual absence of methane from the original gas increases the demand on the methanation section in comparison with processes in which the incoming gas already contains a significant proportion of methane.

Table 1 Gas Compositions and Temperatures in Methanation Process

Position	1	2	3	4	5	6
CO	31.14	14.47	14.47	4.29	4.29	0.34
CO_2	24.66	40.15	40.15	53.93	53.93	62.70
H_2	42.91	35.50	35.50	20.26	20.26	5.83
CH_4	0.08	8.52	8.52	19.84	19.84	29.13
N_2 + Ar	1.21	1.36	1.36	1.68	1.68	2.00
	100.00	100.00	100.00	100.00	100.00	100.00
H_2O	67.3	72.3	72.3	94.4	94.4	118.2
T°C	398	729	325	590	300	428

The process design studied is illustrated in Figure 1, the gas composition and temperature at each stage appearing in Table 1. Incoming gas is mixed with steam (67.3 vols : 100 vols dry gas) and preheated to approximately 400°C at the inlet to the first methanator. Operating pressure is 30 atas (425 psig). The gas leaves the methanator at an adiabatic equilibrium temperature of approximately 730°C, is cooled to 325°C by raising high pressure steam in a boiler and passes to the second methanator. Further methanation occurs and the gas leaves at the adiabatic equilibrium temperature of 590°C. It is again cooled, by raising steam, to 300°C and passes to the final "wet" methanator where it attains an adiabatic equilibrium temperature of about 430°C. At this stage, the gas has a methane content (dry basis) of approximately 29% (78% after CO_2 removal). Subsequent processing stages would include water removal, final "dry" methanation and CO_2 removal to produce the final SNG. Design constraints were incorporated on nickel carbonyl formation in the reactors, which defined the minimum inlet temperatures possible to the first two methanators, and on the amount of steam added which was used to control the maximum temperature in the first methanator below 750°C. Neither the latter, nor the inlet to the third methanator which was arbitrarily set at 300°C, has been rigorously optimised so some flexibility in these values exists.

Catalyst Evaluation

Our previous experience in development and use of catalysts for naphtha- and methane-steam reforming as well as for methanation processes meant that, at the outset of this work, we had "on the shelf" a number of catalysts expected to have activity for the reactions of interest. A laboratory screening test was therefore set up, operating at atmospheric pressure, by which the initial activity of these catalysts could be evaluated rapidly under appropriate conditions of temperature and gas composition. This permitted selection of catalysts for further testing in semi-technical reactors operating under simulated process conditions. Previous experience suggested that provision of a catalyst suitable for the third methanator would present no difficulty so attention was concentrated on the preceding two. In general, steam reforming catalysts were found to lose their low temperature activity relatively rapidly while commercial methanation catalysts were unstable at high temperatures ($>$600°C). However, with experimental preparations it was soon found that low temperature activity was no problem. This allowed evaluations to be performed under first methanator conditions, with the expectation that comparative results would also be valid under second methanator conditions. Numerous catalyst lifetests, of durations varying between one and seventy days, were carried out under these conditions.

In summary, the outcome of the first phase of the catalyst evaluation and development programme was the production of a new high-nickel, co-precipitated formulation (NiO approx 60% loss free) which appeared to have the necessary activity, stability and physical strength for the applications envisaged. When a preferred catalyst formulation had been selected, its preparation was scaled up from the laboratory to a pilot plant located at our catalyst manufacturing site in Clitheroe, Lancashire. This unit is a reduced-scale simulation of a commercial production unit and its use is an essential stage in the development of a procedure for manufacture of a commercial catalyst. Its normal batch size is 15-20 kg and the catalyst manufactured therein was used for all subsequent testing. To demonstrate its properties, three semi-technical reactors were linked in series to permit a long lifetest with the catalyst operating under the conditions of the three methanators.

In common with other nickel-based catalysts, this formulation is susceptible to poisoning by sulphur compounds in the process gas stream. The extent of this was therefore minimised by incorporation of a vessel of desulphurisation catalyst (zinc oxide, ICI catalyst 32-4), upstream of the point of steam addition, running with maximum temperature 250-300°C. By this means, the sulphur level in the process gas was reduced below 0.1 mg S/Nm^3 (dry basis), see below.

The semi-technical reactors used were fabricated from 18/8 Ti stainless steel tube, nominal 1 inch id, overall length 30 ins. The catalyst bed, 12 ins deep, was arranged centrally in the reactor which was also fitted with an internal thermocouple sheath containing six equally-spaced thermocouples positioned throughout the catalyst bed. The reactors were fitted with two external electrical heaters, the first to permit attainment of the selected bed inlet temperature and the second adiabatically controlled to compensate for heat losses. The whole assembly was then surrounded by several inches of inert insulation material. Figure 2 is a simplified illustration of one reactor assembly.

For the performance tests, each reactor was loaded with an undiluted bed, volume 135 ml, of catalyst in the form of pellets diameter 5.4 mm, height 3.6 mm. This was reduced to the active form by passage of pure, dry hydrogen for several hours at 450-500°C and space velocity about 25,000 hr^{-1}. Because these reduction conditions were easily obtained in our equipment, no specific study was made of the reducibility of this catalyst although it has been shown that effectively complete reduction is obtained by passage of hydrogen for two hours at 300°C. After the reduction period, the inlet temperature of each reactor was adjusted to the design setting and the appropriate rate of water fed to the vaporiser upstream of the first methanator. After a few minutes, the hydrogen was replaced by pre-mixed process gas at a flow-rate corresponding to a dry gas space velocity of 10,000 hr^{-1} relative to the catalyst volume in the first methanator. Reduction in dry gas volume through the methanators made the effective (dry) space velocity through the second and third reactors 8865 hr^{-1} and 7160 hr^{-1} respectively. Methanatinn began immediately and steady state conditions in all three reactors were reached within a few hours. The tests were then allowed to run under constant conditions for a prolonged period, catalyst performance being monitored by regular measurement of the temperature profile in each catalyst bed. Outlet gas compositions, which corresponded to the equilibrium composition at each outlet temperature, were monitored by an on-line gas chromatograph.

Figures 3, 4 and 5 show the temperature profiles in each bed at the start of these tests and after continuous operation for the periods indicated. The test ran without significant disturbance for 1500 hrs at which time a plant failure caused an interruption to the water supply and consequently massive carbon deposition in all three reactors. After this upset, it proved impossible to restart the second and third methanators so these were discharged and the catalyst submitted to post-mortem examination. The first methanator was restarted although the temperature profile was found to be displaced substantially down the catalyst bed. Within a few days, however, it recovered to almost its original position (see Figure 3) and then remained stationary until 2200 hrs at

which time the test was terminated.

Post-mortem examination of the catalyst discharged from several levels in each bed revealed that it had mean nickel crystallite sizes in the ranges 750-1000Å, 270-400Å and 160-190Å for the first, second and third methanators respectively. Considering the duration and operating conditions of these tests, this crystallite growth, from an original size of about 100Å, demonstrated the inherent stability towards sintering of this catalyst formulation. Further, the excellent performance during the lifetests showed that this degree of sintering had had no detrimental effect on catalyst activity under the relevant operating conditions. The inference to be drawn is that, with a catalyst of high active metal content operating in a relatively high temperature range, some crystallite growth can be tolerated. The small amount of growth of the catalyst in the second methanator which had run up to 590°C was particularly noteworthy. The results reported were obtained before a full catalyst composition optimisation was carried out. Therefore, although it is not required for these duties, we would expect to be able to design a catalyst with greater resistance to sintering if necessary.

Discharged catalyst from the first two methanators was found to contain sulphur corresponding to an absorption of about 0.015 mg S/Nm^3 of gas passed in the first reactor followed by about 0.065 mg S/Nm^3 in the second, ie a total concentration of 0.08 mg/Nm^3 in the process gas inlet to the first reactor. This concentration caused no significant deactivation of the catalyst in the first bed and a deactivation rate of 1.0-1.5 inches per 1000 hrs in the second which, it is reasonable to postulate, would have been lower at a lower inlet sulphur level. This could have been obtained by optimising the desulphurisation catalyst operating conditions but, in view of the length of test which would have been required to demonstrate an improvement over the performance already observed, this was not felt to be a worthwhile exercise. It will be seen that the distribution of sulphur between the two beds was as would be expected for their inlet and outlet temperatures and the known fact that formation of nickel sulphide is thermodynamically favoured at low temperatures.

DISCUSSION

The catalyst lifetests described above have demonstrated that a formulation has been developed with the activity and stability needed to methanate a variety of process gases at temperatures up to 750°C. By proving the catalyst under simulated process conditions in tests of 2-3 months duration we have been able to show that its rate of deactivation is low enough to be commercially acceptable. Further, by testing under "typical" coal gas methanation conditions, we have acquired the confidence to predict that this catalyst will also perform satisfactorily under the variety of conditions encountered in different proposed coal gas methanation processes. The high temperature capability of this catalyst has the particular advantage of permitting the use of a straight-through methanation system without the need for recycle of product gas for temperature control.

The applicability of this catalyst to processes other than coal gas methanation should also be noted. For example, high temperature methanation steps may be used as sources of heat for steam generation. In such a system, methanatable gas is produced in an endothermic methane-steam reforming stage, piped to the site where the steam is to be generated, methanated, cooled in boilers and feed water heaters, then piped back to the steam reforming stage (4). To use such a process optimally, it is clearly necessary for the methanation catalyst to function over as large a temperature range as possible.

REFERENCES

1 K.H. Eisenlohr, F.W. Moeller and M. Dry in "Methanation of Synthesis Gas," Advances in Chemistry Series 146, 1975, p 113.

2 J.E. Franzen and E.K. Goeke, paper presented at Sixth Synthetic Pipeline Gas Symposium, Chicago, Illinois, October 1974.

3 G.A. White, T.R. Roszkowski and D.W. Stanbridge in "Methanation of Synthesis Gas," Advances in Chemistry Series 146, 1975, p 138.

4 General Electric Co., U.S. patent application no 484802, German OLS 2528660.

FIGURE 1. METHANATION PROCESS

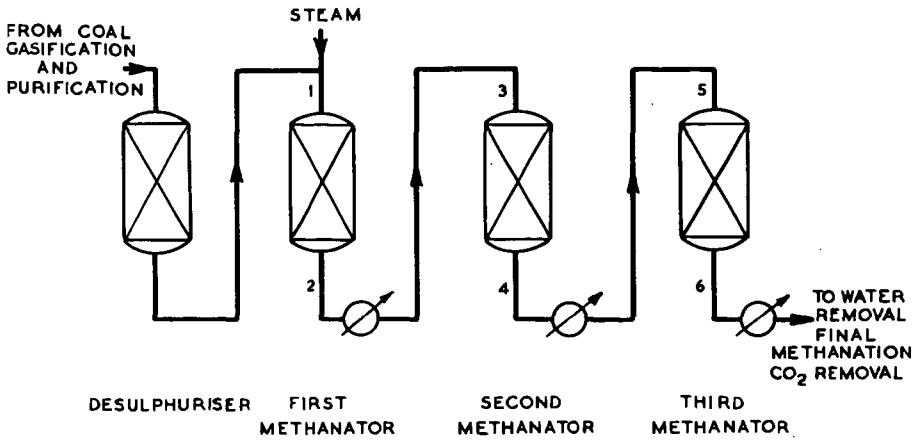

FIGURE 2. METHANATION SEMI-TECHNICAL PLANT REACTOR ARRANGEMENT (SIMPLIFIED)

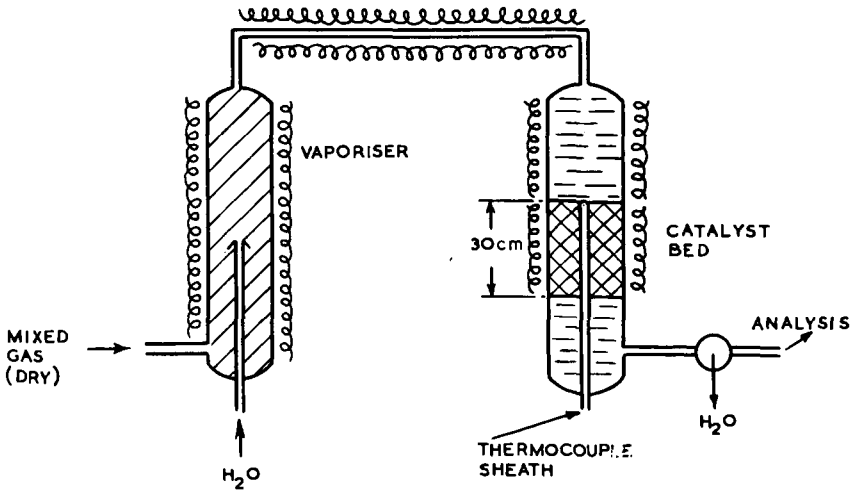

FIGURE 3. FIRST METHANATOR TEMPERATURE PROFILE

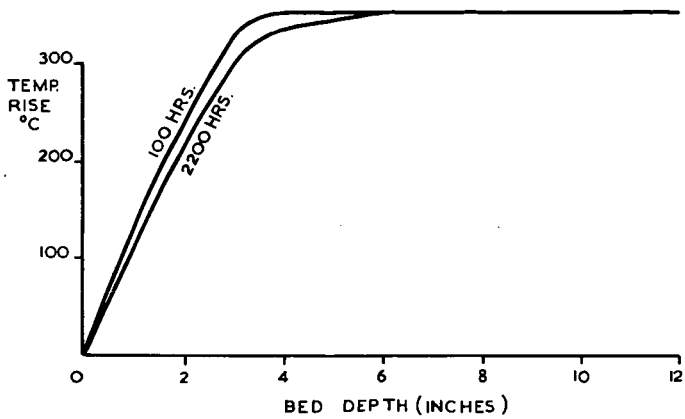

FIGURE 4. SECOND METHANATOR TEMPERATURE PROFILE

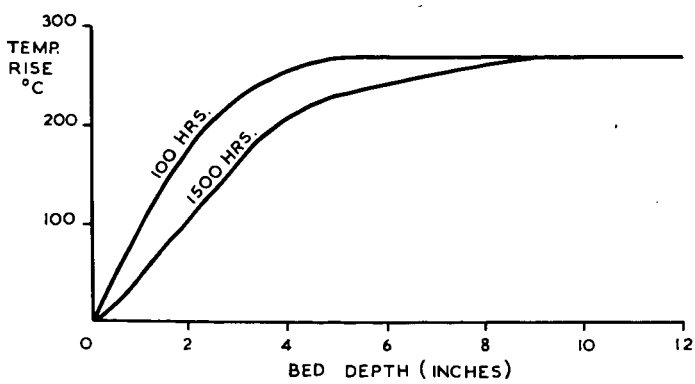

FIGURE 5. THIRD METHANATOR TEMPERATURE PROFILE

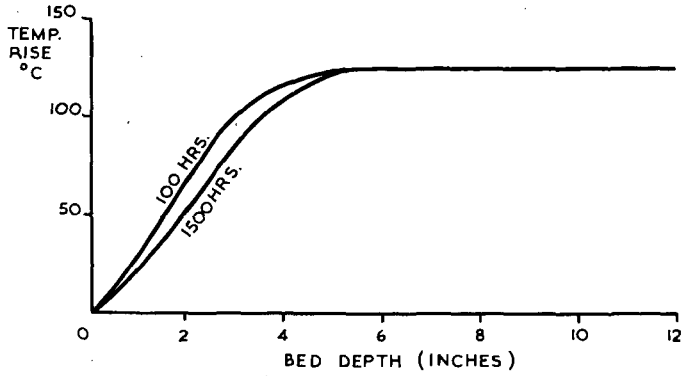

METHANATION ACTIVITY OF SUPPORTED NICKEL ALLOYS

Calvin H. Bartholomew and W. Blaine Barton

Brigham Young University
Department of Chemical Engineering
Provo, Utah 84602

INTRODUCTION

Natural gas is a highly desirable fuel because of its high heating value and nonpolluting combustion products. In view of the expanding demand for and depletion of domestic supplies of clean fuels, economical production of synthetic natural gas (SNG) from coal ranks high on the list of national priorities.

Presently there are several gasification processes under development directed toward the production of methane or SNG. Although catalytic methanation of coal synthesis gas is an important cost item in the process, basic technological and design principles for this step are not well advanced. Extensive research and development are needed before the process can realize economical, reliable operation. Specifically, there appears to be important economic advantages in the development of more efficient, stable catalysts.

Extensive general reviews of pertinent literature dealing with methanation catalysts and kinetics have been provided by Greyson (1) and Mills and Steffgen (2). However, only recently, were kinetic studies of selected Group VIII metals (Fe, Ni, Co, Ru, Rh, Pt, Pd, Ir) reported by Vannice (3,4) and of nickel and ruthenium catalysts by Dalla Betta et al. (5,6) for which the kinetic data were clearly determined under conditions free of heat and mass transfer (diffusional) influences and for which specific rates were based upon active catalytic surface areas.

There is very little mention in previous literature in regard to alloy catalysts for methanation, and no previous kinetic data have been reported for alloy systems. This paper discusses recently determined methanation activity data determined for alumina-supported alloys of nickel with ruthenium, rhodium, molybdenum oxide, iron, cobalt, platinum, palladium and copper. These data were determined under conditions such that effects of heat and mass transfer were minimized and specific rates are reported at 1 atm and 225 and 250°C, based upon active catalytic surface areas.

EXPERIMENTAL

Materials

Analytically pure metal salts (e.g. Baker Analyzed $Ni(NO_3)_2 \cdot 6H_2O$) and Kaiser SAS 5x8 mesh alumina (301 m^2/g) were used in preparation of the supported nickel alloy catalysts. Samples were prepared by simple co-impregnation to incipient wetness of the support with aqueous metal salt solutions followed by oven drying at 80-100°C for 24 hours. The impregnated, dried samples were reduced in flowing hydrogen at 1000-2000 GHSV while heating at less than 5°C/min to 450-500°C with a one hour temperature hold at 230°C and 10-16 hours at 450-500°C. Samples reduced in a separate reduction system were carefully passivated with 1% air in nitrogen before transferring to the reactor.

Hydrogen and nitrogen gases (99.99%) were purified by simultaneously passing both through a palladium Deoxo purifier (Engelhard) and dehydrated molecular sieve or liquid nitrogen trap. Carbon monoxide (Matheson Purity, 99.99%) was used without further purification.

Apparatus and Procedure

Metal surface areas were determined by means of hydrogen chemisorption at 25°C (Ni-Pd at 130°C) using a conventional volumetric apparatus capable of 10^{-6} Torr. Hydrogen adsorption uptakes were determined as a function of pressure and the isotherm was extrapolated to obtain the adsorption at zero pressure. It was assumed that exactly one hydrogen atom adsorbed on each surface metal atom, and site densities were calculated based on the three lowest index planes of each metal (except in the case of Ni-MoO_3 where hydrogen was found to adsorb only on the nickel sites). The surface composition of each alloy was assumed to be the same as the nominal metal composition. Compositions and metal surface areas for catalysts prepared and tested in this study are listed in Table 1.

Methanation activities were measured using a laboratory, single-pass differential flow reactor equipped with Matheson flow meters and pressure regulators, a Hewlett-Packard 7132 temperature recorder, and a Hewlett-Packard 5830 gas chromatograph. A schematic of the reactor system is shown in Figure 1. The stainless steel reactor contained a catalyst chamber of 35cm^3 with adjustable thermocouples installed at each end of the chamber.

Differential activity measurements were carried out at low conversions with 2-4 grams of previously reduced (and passivated) catalyst in the reactor (the remainder of the bed was filled with pure Al_2O_3 pellets) in order to minimize the influence of heat and mass transfer. The sample was heated in flowing H_2 (approximately 500 cm^3/min) to 450°C and held for two hours at that temperature, then allowed to cool in flowing H_2 to about 225°C. Reactant gases (1% CO, 4% H_2 and 95% N_2) were next allowed to flow through the reactor at a space velocity of 30,000 or 60,000 hr^{-1} for 30 minutes during which time the reactor temperature was stabilized at 225, 250, or 275°C. Reactor pressure was usually about 5-8 psig. Three chromatographic samples of the product gas were obtained after which three additional chromatographic samples were taken to determine unconverted reactant gas concentrations. All important experimental conditions such as temperature and pressure were recorded at the time each chromatographic sample was taken.

RESULTS AND DISCUSSION

Methanation activity data in the form of percent CO conversion, CH_4 production, and specific rates are listed for nickel and nickel alloy catalysts in Tables 2-4 (225°C, GHSV = 30,000 and 60,000 hr^{-1} and 250°C, GHSV = 60,000 hr^{-1}) and the specific rates are shown schematically in Figures 2 and 3 for 250°C and GHSV = 30,000 hr^{-1}. For catalysts with low metal loadings, low conversions were obtained. For example, at 250°C (Table 4) conversions for the 3 wt.% catalysts (Ni-A-112, Ni-Ru, Ni-Rh, and Ni-MoO_3) range from 4 to 14% depending upon the space velocity, whereas conversions for the 15 to 20 wt.% catalysts (all other catalysts) range from 11 to 43%. At 225°C the conversion ranges are 4 to 7% and 6 to 35% for low and high metal loadings respectively. Thus, truly differential (low conversion) conditions can be approached at 225°C for the 3% catalysts but not for the 15-20 wt.% catalysts. Apparently then, for our reactor system and for typical methanation catalysts, truly chemically-limited rate data can only be obtained for catalysts with a low metal loading (3-5 wt.%). Accordingly it would be desirable in obtaining very accurate kinetic rate data to prepare all of the catalysts with metal loadings in the 3-5% range. Nevertheless, for purposes of screening, the data obtained at moderate conversions are adequate for comparative purposes.and satisify the objectives of this study.

The turnover numbers (N_{CO} and N_{CH_4}) shown in Tables 2-4 and Figure 3 indicate approximately the same order of magnitude activity for Ni, Ni-Ru, and Ni-Rh catalysts. Our turnover numbers agree well with the initial rates reported by Dalla Betta et al. (5) and Vannice (3) for 0.5% Ru/Al_2O_3 and 5% Ni/Al_2O_3. It

appears that a small uncertainty (1-5%) in our results may be attributed to small variations in gas concentrations, pressure and flow rates over the test period of a given catalyst. The measurement of both activity and selectivity also includes uncertainties of 1-5% in calibration and measurement of gas concentrations. Thus, it may be possible that selectivities for CH_4 are slightly higher than indicated, although there is undoubtedly significant hydrocarbon and CO_2 production (3, 5).

Dalla Betta et al. (6) have indicated that their steady-state rates for methanation (after a 24-hour exposure to a reaction mixture) are 25 times lower than their initial rates (5). Thus, exposure to a reaction mixture over a period of hours or even minutes may significantly reduce the activity of the catalyst. This may explain why the turnover numbers reported in this study which were measured after exposure for 1/2 to 4 hours under reaction conditions are significantly lower than initial rates reported in the literature for 5% Ni/ZrO_2 (5) and 5% Ru/Al_2O_3 (3). The discrepancy between initial rates measured by Dalla Betta (5) and Vannice (3) for nickel and ruthenium catalysts might be similarly explained by differences in their pretreatment of the catalyst. Also, Vannice based his turnover numbers on CO adsorption data, which in fact may explain differences of 100-400% between his data and ours or those of Dalla Betta.

Vannice (3) has reported selectivities for the methanation reaction over the group VIII metals to be in the following decreasing order: Pd>Pt>Ir>Ni>Rh>Co>Fe>Ru. This order correlates well with measured selectivities for alloys of these same metals with nickel as shown in Tables 2-4. Of special interest is Ni-Pt-A-100 which shows the highest selectivity, 99% at 250°C and higher temperatures. Changes in space velocity and temperature have appreciable effects on the selectivity as can be seen for example in the data for Ni-A-112, Ni-Pd-A-100 and Ni-Ru-A-105. Generally the selectivity increases with increasing temperature for a given space velocity and with increasing space velocity for a given temperature.

Figures 2 and 3 illustrate the magnitude of the rates per gram of catalyst, the turnover numbers, and selectivities at 250°C and a space velocity of 30,000 hr^{-1}. Nominal compositions and hydrogen uptakes used to calculate turnover numbers are listed in Table 1. It should be observed that the active metal loadings which vary significantly between catalysts have an obviously marked effect on the activity of the catalyst per unit catalyst weight as can be seen in Figure 2 where the listed order corresponds to the order of wt.% active metal. A comparison of these rates with the hydrogen uptake data shows that the rate is strongly influenced by the available surface area. For example, Ni-A-116 (14 wt.% Nickel) is more active (per unit mass) than G-87 (32 wt.% nickel) mainly because the surface area of the former catalyst is larger.

Turnover numbers for 250°C and a space velocity of 30,000 hr^{-1} are shown in decreasing order of activity in Figure 3. Ni-MoO_3-A-101, Ni-A-112 (3% nickel) and Ni-Co-A-100 are the most active and G-87 the least active. The details of these results are discussed below for each catalyst.

Ni-MoO_3-A-101 has a relatively low active surface area. Thus, its rate per unit weight is among the lowest tested. However, its turnover number is the highest of any catalyst tested. Assuming a method to increase the active surface area can be found, this catalyst is a most promising candidate for further study.

Ni-Ru-A-105 and Ni-Rh-A-100 behave typically as nickel catalysts showing comparatively little effects of alloying although both are slightly less active than Ni-A-112, a nickel catalyst of comparable weight loading. The Rh does cause some increased selectivity to methane but not as pronounced as for platinum. The data determined at 225°C (Table 2) show an unexpectedly low selectivity to methane for Ni-Rh. Thus, some of this work will be repeated.

Ni-Co-A-100 contains a high loading of metal with equal weight percents of nickel and cobalt. It is of special interest in that both the rate per unit weight and the turnover number are high. The selectivity of this catalyst for the methanation reaction (78% at 250°C and GHSV = 30,000) is the lowest of any nickel catalyst tested. Vannice (3) has reported cobalt to have a selectivity of 78% under similar reaction conditions and the selectivity for nickel to be 90% also in good agreement with our data. Thus, cobalt has a strong effect on the selectivity of the Ni-Co catalyst. Nevertheless, a recent test showed the same catalyst to have a 93.5% selectivity at 225°C and GHSV = 30,000 hr^{-1}. Since the selectivity should be lower at 225 than at 250°C, these data must be repeated.

Ni-Fe-A-100 was found to completely deactivate within two hours under normal reactor operating conditions. When the catalyst was removed from the reactor some of the beads showed a brown (rust) color as compared to the normal black. The observations suggest that the iron may scavange the oxygen from the CO to form various iron oxides and thus effectively poison the catalyst. It is also possible that the Ni-Fe catalysts was not completely reduced at the beginning of the test. Additional reactor tests are planned to investigate these possibilities.

Ni-Pd-A-100 was found to be less active than most of alloys tested thus far with a turnover number about the same as G-87. Ni-Pt-A-100 has rate characteristics which are not outstandingly different from the other catalysts. The selectivity, however, is significantly improved over nickel. Vannice (3) has shown platinum to be one of the most selective catalysts for methane--namely about 98% to CH_4. As an alloy with nickel in the amount of only one atomic percent platinum effects a 99% selectivity to methane.

Ni-A-116 is a high loading (15 wt.%) nickel catalyst used to compare against other catalysts containing 15-20 wt.% alloy. It has the highest rate per unit weight but has a turnover number the same as Ni-Pt-A-100 and somewhat lower than the cobalt alloy.

G-87 is a commercial nickel catalyst manufactured by Girdler Catalyst Corp. and is included as a comparison against other nickel catalysts. It is unique, however, from the other catalysts tested because it contains a different support of unknown composition which may influence the diffusional and mass transfer characteristics of the catalyst. Because of its high nickel loading (32 wt.%) it is expected that its rate per unit weight should be high. However, its turnover number is one of the lowest measured. This may be due in part to the effects of pore diffusion resistance at a relatively high conversion of CO.

Data on Ni-Cu-A-100 obtained at 250°C and a space velocity of 30,000 hr^{-1} show this to be the least active catalyst tested thus far with relatively low selectivity. No further work is expected to be done with this catalyst because of its low activity.

Apparent activation energies for some of the nickel-alloy catalysts are listed in Table 5. With the exceptions of Ni-MoO_3-A-101, Ni-Co-A-100, and Ni-Rh-A-100, the catalysts appear to have activation energies of 12-18 kcal/mole for both CO conversion and methane formation. Ni-Co-A-100 and Ni-Rh-A-100 have slightly higher values of 22.2 and 19.2 respectively. Ni-MoO_3-A-101 has a significantly higher value of 26 kcal/mole which is close to the value of 25 kcal/mole for nickel reported by Vannice (3). The far right column lists the activation energies for various metals as reported by Vannice and measured under kinetic limited (low conversion) conditions. Considerably lower activation energies for alloys compared to those of either alloy component very likely result at least in part from mass transfer (or diffusional) limitations. In addition, the variations are partly the result of alloy formation, the alloy having catalytic properties different from either of the pure metals.

CONCLUSIONS

1. Steady-state conversions of carbon monoxide at 225 and 250°C, 1 atm. (inlet composition of 1% CO, 4% H_2, 95% N_2) range from 3-43% for alumina-supported nickel alloy catalysts. Percent selectivities to methane range from 67-99%. Turnover numbers are not significantly different within experimental error for Ni-Rh, Ni-Ru, and Ni catalysts and compare favorably with initial rates reported for 5% Ni/Al_2O_3 and 0.5% Ru/Al_2O_3.

2. Steady-state conversion measured at 225 and 250°C, 1 atm and for space velocities of 30,000 and 60,000 hr^{-1} indicate that very nearly differential (low conversion) conditions obtain only for low (3-6 wt.%) metal loading catalysts. Screening data for 15-20 wt.% metal/Al_2O_3 catalysts are influenced by mass transfer or diffusional limitations.

3. $Ni\text{-}MoO_3/Al_2O_3$ is the most active catalyst on a per surface area basis. Ni-Pt/Al_2O_3 has the highest selectivity for methane production--namely 99% (250°C, 30,000 hr^{-1}). A 14 wt.% Ni/Al_2O_3 is the most active catalyst on a per mass basis--even more active than a commercial 32 wt.% Ni/Al_2O_3 simply because the 14% catalyst has a high nickel surface area.

REFERENCES

1. M. Greyson, "Methanation" in "Catalysis" Vol. IV, ed. P.H. Emmett, Rheinhold Pub. Corp., New York, 1956.

2. G.A. Mills and F.W. Steffgen, "Catalytic Methanation," Catalysis Reviews 8, 159 (1973).

3. M.A. Vannice, "The Catalytic Synthesis for Hydrocarbons from H_2/CO Mixtures over the Group VIII Metals," J. Catal, 37, 449 (1975).

4. M.A. Vannice, "The Catalytic Synthesis of Hydrocarbons from H_2/CO Mixtures over the Group VII Metals, III. Metal-Support Effects with Pt and Pd Catalysts," J. Catal. 40, 129 (1975).

5. R.A. Dalla Betta, A.G. Piken, and M. Shelef, "Heterogeneous Methanation: Initial Rate of CO Hydrogenation on Supported Ruthenium and Nickel," J. Catal, 35, 54 (1974).

6. R.A. Dalla Betta, A.G. Piken, and M. Shelef, "Heterogeneous Methanation: Steady State Rate of CO Hydrogenation on Supported Ruthenium, Nickel, and Ruthenium," J. Catal. 40, 173 (1975).

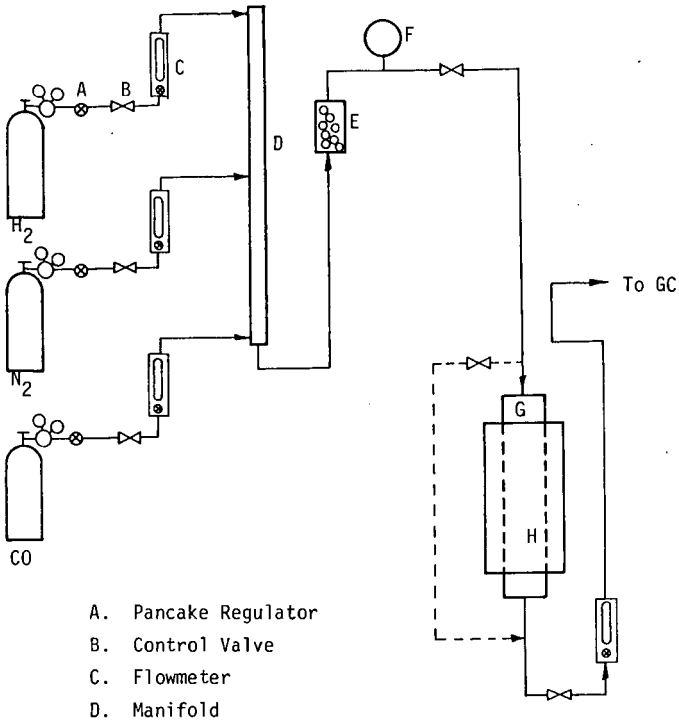

A. Pancake Regulator
B. Control Valve
C. Flowmeter
D. Manifold
E. Mixing Chamber
F. Pressure Gauge
G. Reactor
H. Furnace

Figure 1 Low Pressure Continuous Flow Reactor System for Methanation Studies

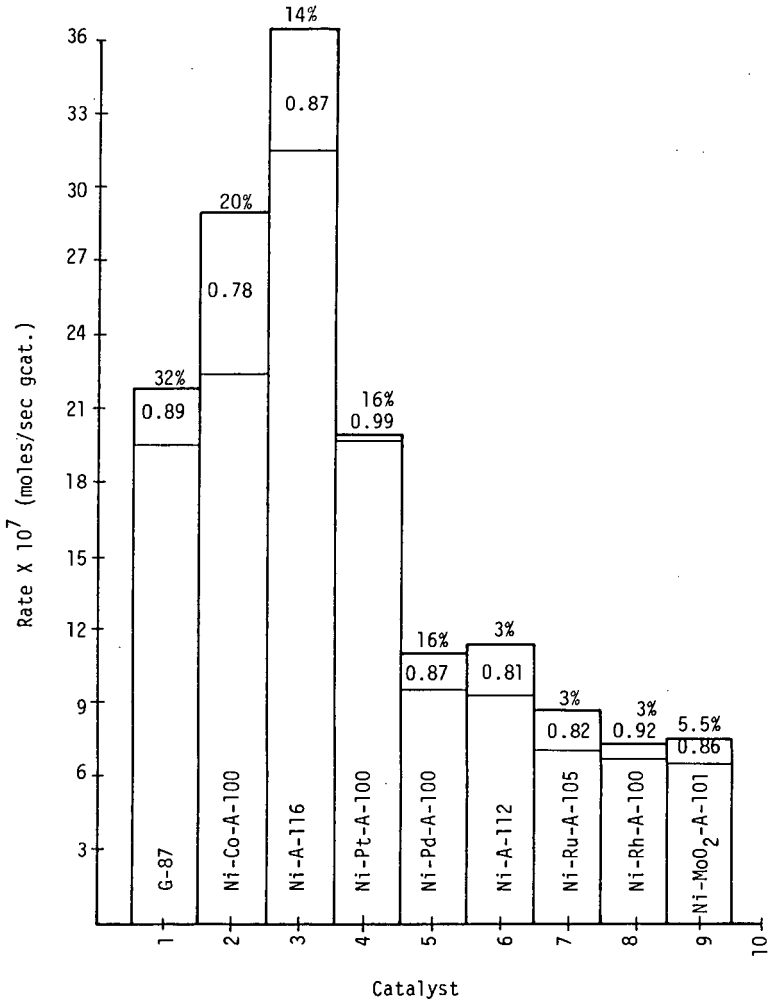

Figure 2 Specific Methanation Rates (mass basis) for Nickel and Nickel Alloy Catalysts. (Percentages are active metal loadings. Fractions represent selectivity to methane.) (T=250°C; GHSV=30,000 hr^{-1})

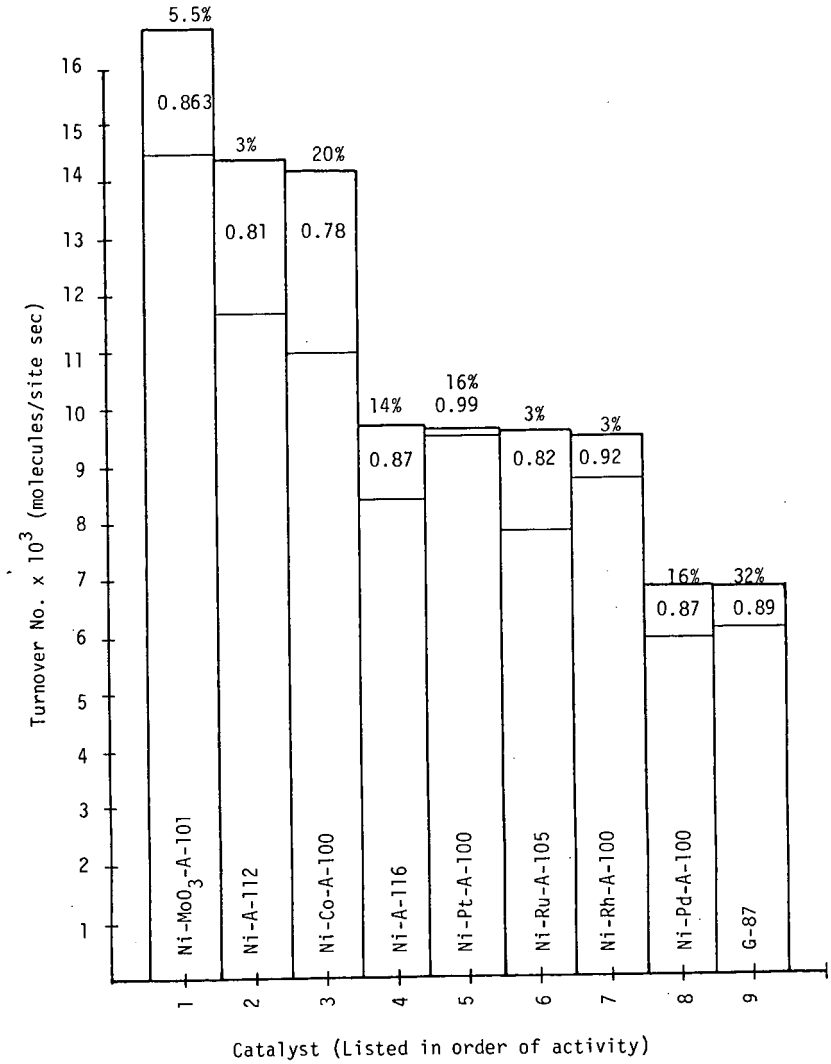

Figure 3 Turnover Numbers (molecules product/site sec) for Methanation on Nickel and Nickel Alloy Catalysts. (Percentages are active metal loadings. Fractions represent selectivity to methane.) (T=250°C; GHSV=30,000 hr^{-1})

TABLE 1

Hydrogen Chemisorptive Uptake Data for Alumina-Supported Nickel Nickel Alloy and Ruthenium Alloy Catalysts

Catalyst	Nominal Composition (wt%)	H_2 Uptake (μmoles/gram)	Metal Particle Size (A)	Percent Dispersion	Surface Area (m^2/g)
Ni-A-111	3% Ni	21.4	116	8.35	1.75
Ni-A-112	3% Ni	39.4	63	15.4	3.23
Ni-A-116	14% Ni	187.8	62	15.7	15.39
G-87 (Girdler)	32% Ni	161.6	163	5.93	13.24
Ni-MoO_3-A-101	2.5% Ni - 3% MoO_3	22.5	92*	10.6*	1.84*
MoO_3-A-101	3% MoO_3	1.0	--	--	--
Ni-Ru-A-105	2.5% Ni - 0.5 wt% Ru	44.6	52	18.76	3.71
Ni-Rh-A-100	2.5% Ni - 0.5% Rh	38.3	62	16.1	3.16
Ni-Co-A-100	10% Ni - 10% Co	114.9	142	6.76	9.54
Ni-Fe-A-100	10% Ni - 10% Fe	80.6	278	4.60	5.14
Ni-Pt-A-100	15.7% Ni - 0.5% Pt	106	119	8.22	8.66
Ni-Pd-A-100	15% Ni - 1.0% Pd	107.4	115	8.13	8.82

* Based upon nickel only

TABLE 2 Reactor Screening Data for Nickel and Nickel Alloy Catalysts
225°C, GHSV = 30,000 hr^{-1}, 16 psia

Catalyst	Conversion CO	Production CH_4	Production Other	Rate x 10^7 ($\frac{mole}{g\ sec}$) CH_4	Rate x 10^7 ($\frac{mole}{g\ sec}$) CO	Turnover # x 10^3 (sec^{-1}) CH_4	Turnover # x 10^3 (sec^{-1}) CO	Selectivity to CH_4
Ni-Co-A-100	16.2	15.15	1.05	9.31	9.96	4.56	4.88	0.935
Ni-Pt-A-100	16.77	15.20	1.60	9.91	10.95	4.77	5.27	0.906
Ni-Ru-A-105	5.18	3.48	1.73	2.79	4.17	3.12	4.68	0.672
Ni-Rh-A-100	3.3	2.2	1.1	1.48	2.21	1.93	2.88	0.671
Ni-Pd-A-100	6.9	6.67	0.2	4.62	4.79	2.87	2.97	0.97
Ni-MoO_3-A-101	2.9	2.5	0.4	1.83	2.11	4.07	4.69	0.87
Ni-Fe-A-100	De-activates under reaction conditions							
G-87	22.45	19.55	2.88	9.81	11.25	3.04	3.49	0.871
Ni-A-112	6.63	4.47	2.13	3.62	5.35	4.60	6.80	0.674
Ni-A-116	34.63	28.08	6.55	19.23	23.74	5.13	6.32	0.815

TABLE 3 Reactor Screening Data for Nickel and Nickel Alloy Catalysts
225°C, GHSV = 60,000 hr^{-1}, 20 psia

Catalyst	% Conversion CO	% Conversion CH_4	% Production Other	Rate x 70^7 (mole/g sec) CH_4	Rate x 70^7 (mole/g sec) CO	Turnover # x 10^3 (sec^{-1}) CH_4	Turnover # x 10^3 (sec^{-1}) CO	Selectivity to CH_4
Ni-Co-A-100								
Ni-Pt-A-100	15.53	14.03	1.43	18.47	20.33	8.88	9.80	0.903
Ni-Ru-A-105	4.15	3.25	0.88	5.23	6.63	5.87	7.44	0.788
Ni-Rh-A-100								
Ni-Pd-A-100	6.63	5.43	1.23	7.76	9.49	4.81	5.89	0.817
Ni-MoO_3-A-101	3.70	3.03	0.67	4.84	5.86	10.74	13.03	0.827
Ni-Fe-A-100			De-activates under reaction conditions					
G-87	20.37	17.43	2.93	18.53	21.63	5.75	6.72	0.856
Ni-A-112	5.70	4.63	1.03	7.12	8.71	9.04	11.05	0.812
Ni-A-116	24.05	21.98	2.05	30.88	33.76	8.47	8.99	0.914

TABLE 4 Reactor Screening Data for Nickel and Nickel Alloy Catalysts
250°C, GHSV = 60,000 hr^{-1}, 20 psia

Catalyst	% Conversion CO	% Production CH_4	% Production Other	Rate x 10^7 (mole/g sec) CH_4	Rate x 10^7 (mole/g sec) CO	Turnover # x 10^3 (sec^{-1}) CH_4	Turnover # x 10^3 (sec^{-1}) CO	Selectivity to CH_4
Ni-Co-A-100	38.7	30.43	8.27	38.03	48.3	18.6	23.7	0.787
Ni-Pt-A-100								
Ni-Ru-A-105	9.47	8.03	1.47	12.70	14.97	14.20	16.80	0.848
Ni-Rh-A-100								
Ni-Pd-A-100	11.2	10.3	0.9	14.67	15.93	9.09	9.85	0.92
Ni-MoO_3-A-101	9.3	8.7	0.65	13.56	14.58	30.14	32.41	0.92
Ni-Fe-A-100			De-activates under reaction conditions					
G-87								
Ni-A-112	14.43	13.58	0.88	20.64	21.99	26.19	27.91	0.941
Ni-A-116	43.53	38.17	5.43	53.38	60.94	14.21	16.22	0.877

TABLE 5 Apparent Activation Energies for Methanation Catalysts
Based on measurements at 225-250°C and a space velocity of 30,000 hr^{-1}

Catalyst	CO Conversion (Kcal/mole)	CH_4 Production (Kcal/mole)	Metal*	CH_4* Production Kcal/mole
Ni-Co-A-100	22.2	18.3	Co	27.0±4.4
Ni-Pt-A-100	12.4	14.3	Pt	16.3±0.8
Ni-Ru-A-105	14.8	19.0	Ru	24.2±1.2
Ni-Rh-A-100	19.2	21.1	Rh	24.0±0.4
Ni-Pd-A-100	17.1	14.8	Pd	19.7±1.6
Ni-MoO_3-A-100	26.2	26.2		
Ni-Fe-A-100			Fe	21.3±0.9
G-87	13.7	14.2	Ni	25.0±1.2
Ni-A-112	15.5	19.2		
Ni-A-116	8.8	10.2		

*Data of Al Vannice (Exxon) Ref.

HETEROGENEOUS METHANATION:

EFFECTS OF CARBON, SULFUR AND WATER

ON ACTIVITY MEASUREMENTS AT VARIOUS TEMPERATURES

R. A. Dalla Betta(*) and M. Shelef
RESEARCH STAFF
FORD MOTOR COMPANY
P. O. BOX 2053, DEARBORN, MI 48121

INTRODUCTION

A wide variety of experimental procedures has been used to measure catalytic activity and to compare catalysts for carbon monoxide hydrogenation. The comparison is generally carried out in flow reactors operating at high conversions. While such conditions are more realistic and may better duplicate catalyst performance in actual use, specific catalyst activities or specific reaction rates are difficult to estimate from such data. This is especially true for highly exothermic reactions such as CO hydrogenation where the temperature as well as concentrations change along the catalyst bed. Sulfur tolerance tests generally took the form of sulfidation capacity measurements with the sulfur being quantitatively taken up by the catalyst bed.

The first publications of this series presented data on initial reaction rates (1) on clean metal surfaces and on steady-state rates (2) on several catalysts both in sulfur-free and sulfur containing streams. In this paper a series of Ni catalysts is compared in several different tests. It will be demonstrated that conclusions derived from steady-state rates at 673 K are markedly different from those drawn at 523 K. Similar contradictions apply to tests designed to assess the activity in the presence of sulfur. Water vapor in the reactant stream is found to have a significant effect on both the high temperature steady-state activity and the final activity in the presence of sulfur.

EXPERIMENTAL

1. Apparatus

Initial rates were measured in a Pyrex glass batch recycle system as described previously (1). The reactor loop was filled with the reactants to the required pressure and mixed by circulating through a bypass. The catalyst sample was reduced in a stream of flowing hydrogen, cooled to the reaction temperature, evacuated and the reactants diverted over the catalyst. Samples of the reactant gas were analyzed by injection into a gas chromatograph equipped with a flame ionization detector. Both methane and total hydrocarbons were determined, steady-state rates were

(*) Current Address: Catalytica Associates, 2 Palo Alto Square, Palo Alto, California 94304

measured in an atmospheric pressure single pass flow reactor, also described previously (2). The flow of each reactant was set by controlling the upstream pressure on a stainless steel capillary. The catalyst was contained in a Pyrex reactor supported on a porous glass disc. The reactor effluent was analyzed as described above.

Water was introduced into the reactant stream through a Pyrex tube extending into the glass reactor and connected to a motor driven positive displacement syringe pump. The pump was constructed of stainless steel and had a volume of 500 cc. The inlet portion of the reactor, including a plug of glass wool, was heated resistively to vaporize the water. The pressure of water in the reactant stream was controlled by the pump speed which was set at 0.049 cc/min.

2. Materials

The catalysts have been described in detail in previous publications (1,2). The supported catalysts were prepared by impregnation of the oxide support with aqueous $Ni(NO_3)_2$ solution. The 5% Ni/ZrO_2 (I) (1) and 5% Ni/ZrO_2 (II) (2) were prepared from different batches of ZrO_2 obtained from the TAM Division of National Lead Co. This material was found to be quite impure, containing appreciable amounts of Cl, Ca, Mg, Fe and Hf (3). These batch to batch variations may, possibly explain some of the activity differences observed in the catalysts made with the ZrO_2 support. Raney Ni was prepared by extraction of a 50:50 Ni/Al alloy with NaOH to dissolve 60% of the Al. Hydrogen adsorption isotherms were determined on these catalysts (2) and the results are collected in Table 1.

RESULTS

After reduction of the catalyst at 723 K, initial reaction rates were measured on the clean metal surface using the batch recycle reactor. Reactant composition was $P(H_2)$ 0.5625 atm and P(CO) 0.1875 atm. The rate was calculated from conversion versus time data at short times (1). The system is well-behaved as shown by a typical set of data for 2% Ni/Al_2O_3 presented in Fig. 1. Results for a number of Ni catalysts are collected in Table 2.

Steady-state rates were measured in the single pass flow reactor at atmospheric pressure with a reactant stream composition of $P(H_2)$ 0.5938, P(CO) 0.1562, and P(He) 0.250 atm, corresponding to an H_2/CO ratio of 3.8. After the catalyst was reduced at 723 K, the temperature was lowered to 523 K and the reactants diverted over the sample. Steady-state was usually attained after 6 to 8 hrs. but 24 hrs. were allowed to elapse before at least four gas samples are analyzed and averaged to determine the catalyst activity. Then, 10 ppm H_2S was introduced into the reactant stream, and after 24 hrs., the activity again determined. In a similar manner, the H_2S flow was stopped and the activity recovery, if any, noted. These results are presented in Fig.2. In Fig.3 the catalyst activities are compared at 673 K. The procedure used in this case was to start the reactants over the samples at 520 to 550 K then slowly heat the samples to 673 K without exceeding a turnover number of 0.2/s. As before, 24 hrs. elapsed at each condition before activity data were taken.

Up to this point the activity measurements have been run without the addition of water. Although water is a reaction product, the differential conditions of the flow reactor experiment keep the partial pressure of water over the catalyst low.

In Figs.4 and 5 there are, respectively, collected steady-state results from runs in which water was added to the reactant stream for the 5% Ni/ZrO_2 (II) and 2% Ni/Al_2O_3 catalysts. The conditions at which each of the rate measurements, shown in Figs.4 and 5, were made are given in Table 3. Following a procedure similar to the previous measurements, the catalysts were reduced at 723 K, cooled to 523 K and the flow of CO and H_2 started. Data at condition A were obtained after 24 hrs. Water was then injected and 24 hrs. later the reaction rate was measured. Similarly, each subsequent data point was taken after waiting 24 hrs. for steady-state conditions to be established.

DISCUSSION

1. Steady-State Activity

Comparison of the initial rate data (Table 2) and the steady-state data at 523 K (Fig.2) shows that at this temperature the steady-state surface is similar, or at least has comparable catalytic activity to the clean metal surfaces studied by initial rate measurements. The relative ordering of the activity of the three catalysts is the same from either set of data. When the catalysts are heated to 673 K and again compared (Fig.3), the activity is significantly reduced in comparison to the rate expected from extrapolation according to the measured activation energy (Table 2). The activity is lower by a factor of approximately 30, indicating a surface deactivated by carbonaceous deposits either as a carbon overlayer or by the formation of a carbide-like species (2). Although the results presented here are at 673 K, it should be noted that the deactivation was observable at even lower temperatures and varied in its rate of approach to steady-state from one catalyst to another. A quantitative indication of this phenomenon is presented in Fig.6. After reduction, the catalyst was cooled to the temperature at which the initial rate was expected to be either 0.1 or 0.01 per second, and the reactants were passed over. The temperature was then adjusted to maintain a nearly constant turnover number. The Raney Ni at a specific rate of 0.01/s, corresponding to a temperature of 483 K, shows no apparent deterioration in activity after 5 days. At a temperature of 548 K and an activity of 0.1/s, the activity constantly decreased. To maintain a constant activity it was necessary to continuously raise the temperature. The rate of deactivation was observed to accelerate as the temperature was raised, as seen by the accelerating slope of the curve in Fig.6. The rate of activity deterioration appeared also to be dependent on the support, 5% Ni/ZrO_2 deteriorating much more rapidly than 2% Ni/Al_2O_3 or Raney Ni. The deterioration is not associated with thermal sintering of the Ni, since it was shown earlier that cleaning the catalyst of carbon could restore the higher activity (2).

As a result of this different susceptibility to deactivation by carbon overlayer formation at different temperatures the relative specific activity of a series of catalysts at steady state can be completely reversed at different test temperatures. At 523 K the relative activity is 5% Ni/ZrO_2 (II) > 2% Ni/Al_2O_3 > Raney Ni, while at 673 K the order is Raney Ni > 2% Ni/Al_2O_3 > 5% Ni/ZrO_2 (II).

2. Sulfur Poisoning

The temperature chosen for sulfur poisoning studies is also extremely important. At 523 K the deactivation is a factor of 170 in the best case, Raney Ni, while it is only 2.5 for 5% Ni/ZrO_2 (II) at 673 K. This decreased poisoning at

higher temperatures is consistent with the decreased stability of the sulfide. The ordering of the catalysts is substantially different, 2% Ni/Al_2O_3 showing the greatest susceptibility to poisoning at 523 K, while Raney Ni is most susceptible at 673 K. Such large changes in the ordering of catalyst sensitivity to sulfur, at least in this type of test, implies complex behavior. For example, at low temperatures, the presence of sulfur leads to the formation of a bulk metal sulfide (4) and the effect of the support may be to inhibit the formation of such sulfides. At higher temperatures other compounds may form such as sulfospinels in the case of the Raney Ni which contains elemental Al (2).

The H_2S pressure is too low to form a bulk sulfide at 673 K (4) and a surface sulfur layer may have to compete with the carbon containing layer that apparently forms at this temperature. This is in apparent agreement with the observation that the least active catalysts in sulfur-free environment at 673 K are the most active in the presence of H_2S.

3. Effect of H_2O

Yet another measurement procedure to compare catalysts for CO hydrogenation includes H_2O in the reactant stream at the catalyst inlet. Inclusion of a large partial pressure of water would more closely simulate the industrial process since water is purposely added to reduce carbon formation in the reactor and to generate hydrogen by the water gas shift reaction. The data of Figs.4 and 5 show that at 523 K water has an inhibiting effect. At 673 K, however, 5% Ni/ZrO_2 (II) and 2% Ni/Al_2O_3 behave quite differently in the presence of H_2O. The ZrO_2 supported catalyst shows inhibition by water (compare arrow - water free data from Fig.3), while 2% Ni/Al_2O_3 is substantially more active. The latter behavior is expected if it is assumed that the high temperature deactivation is due to carbon and that the presence of water inhibits carbon formation. The thermodynamic inhibition of carbon formation by water is well known (5). The behavior of 5% Ni/ZrO_2 (II) is difficult to explain.

When H_2S is added to the reactant stream, the 2% Ni/Al_2O_3 catalyst becomes totally inactive (Fig.5), the conversion being below the detection limit of the analytical system. The 5% Ni/ZrO_2 (II) is only slightly more active. The comparison of the effect of 10 ppm H_2S in a dry stream and in a reactant stream containing 13 mol% water reveals the significant impact water can have on the measured "sulfur resistance" of a catalyst. Whereas 5% Ni/ZrO_2 (II) appeared to deteriorate by only a factor of two with 10 ppm H_2S, the combination of water and 10 ppm H_2S results in a deterioration greater than 100-fold. When both the water and the H_2S were removed from the reactant stream, the activity recovered but for 5% Ni/ZrO_2 the highest recovery was obtained in a stream containing sulfur. In fact, with the system at reaction conditon D, i.e. both H_2O and H_2S in the reactant stream, removing the H_2O but keeping the H_2S in the reactant stream results in an increase in catalyst activity by two orders of magnitude. This behavior was completely reversible; the catalyst could be cycled between conditions D, E and G of Table 3 repeatedly without adverse effects.

The behavior described above emphasizes the importance of water when searching for sulfur resistant catalysts. But even more significantly it may give clues to the properties desired in a sulfur resistant methanation catalyst. The formation of a material stable toward reaction with H_2S is one route to sulfur resistance if this phase possesses some catalytic activity (6). The carbon containing phase may be such a material. A significant partial pressure of water may reduce its stability, permitting the inactive sulfide phase to form.

The measured specific activity and the relative ordering of CO hydrogenation catalysts can vary markedly depending on the temperature and reactant stream composition chosen for the catalytic test. Low temperature tests employing either initial or steady-state rate measurements, give activity data for a clean metal surface. Results obtained at 673 K apparently are representative of a carbon contaminated surface.

The choice of the test temperature and reactant stream composition is extremely important in designing an experimental test for catalyst resistance to sulfur poisoning. Water should be added to the reactant stream since it has a great effect on the sulfur tolerance of Ni catalysts.

REFERENCES

1. R. A. Dalla Betta, A. G. Piken, and M. Shelef
   J. Catal. 35, 54 (1974).
2. R. A. Dalla Betta, A. G. Piken, and M. Shelef
   J. Catal. 40, 173 (1975).
3. M. Bettman, Research Staff, Ford Motor Co, unpublished results.
4. T. Rosenquist, J. Iron and Steel Inst.176,37 (1954).
5. G. A. White, T. R. Roszkowski, and D. W. Stanbridge,
   Am. Chem. Soc., Div. Fuel Chem. Preprint 19 (3) 57 (1974).
6. M. Boudart, J. A. Cusumano, and R. B. Levy
   New Catalytic Material for the Liquefaction of Coal,
   Report RP-415-1, Electric Power Research Institute, October 30,(1975).

TABLE 1

Hydrogen Adsorption Results

Catalyst	H_2 Adsorption μmol/g	Dispersion H (ads)/M(tot)
5% Ni/ZrO_2 (I) (*)	33.7	0.079
5% Ni/ZrO_2 (II) (**)	19.2	0.045
2% Ni/Al_2O_3	5.6	0.033
Raney Ni	137	0.031

(*) Sample used in ref (1)
(**) Sample used in ref (2)

TABLE 2

Initial Rates of CO Hydrogenation (*)

Sample	N at 523 K s^{-1} x 100		E_a kcal/mol	
	HC(total)	CH_4	HC(total)	CH_4
5% Ni/ZrO_2 (I)	6.3	2.3	20	28
5% Ni/ZrO_2* (II)	27	9.6	30	33
2% Ni/Al_2O_3	5.1	2.0	30	31
Raney Ni	3.2	1.0	26	31

(*) $P(H_2)$ 0.5625 atm., P(CO) 0.1875 atm.

TABLE 3

Reaction Conditions at Steady-State for Runs in Figures 4 & 5

Reactions Conditions(*)	Temp (K)	Reactant Composition (Atm)				
		H_2O	H_2S	H_2	CO	He
A	523	0	0	0.5938	0.1562	0.250
B	523	0.133	0	0.515	0.135	0.217
C	673	0.133	0	0.515	0.135	0.217
D	673	0.133	10-5	0.515	0.135	0.217
E	673	0.133	0	0.515	0.135	0.217
F	673	0	0	0.5938	0.1562	0.250
G	673	0	10-5	0.5938	0.5938	0.250

(*) The conditions were maintained for 24 hrs before the steady-state reaction rate was determined.

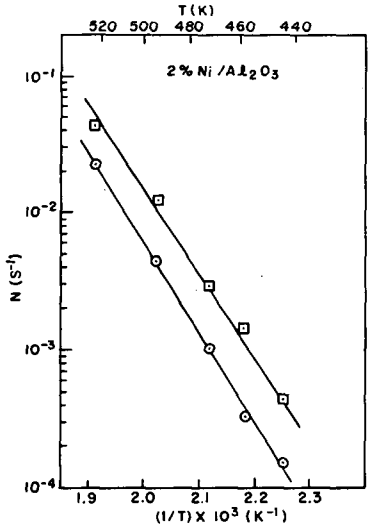

FIG. 1

Initial rate of CO hydrogenation on 2% Ni/Al_2O_3. □ - Total hydrocarbon synthesis rate; O - CH_4 synthesis rate.

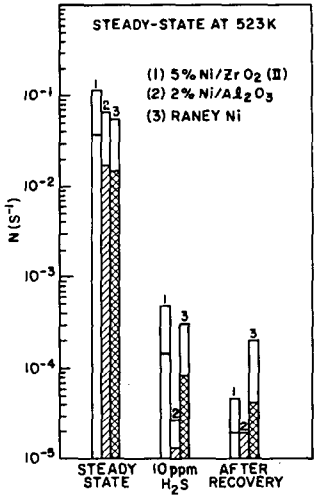

FIG. 2

CO hydrogenation at 523K on (1) 5% Ni/ZrO_2(II); (2) 2% Ni/Al_2O_3; (3) Raney Ni.

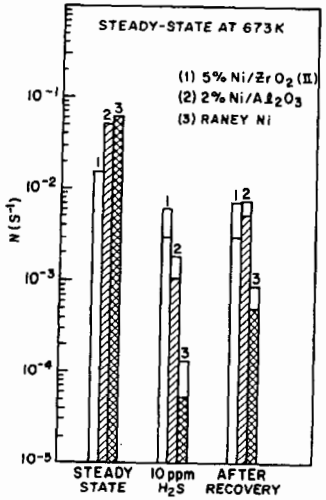

FIG. 3

CO hydrogenation at 673K on (1) 5% Ni/ZrO_2(II); (2) 2% Ni/Al_2O_3; (3) Raney Ni.

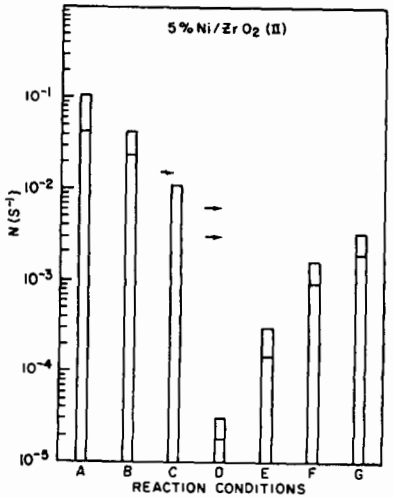

FIG. 4

CO hydrogenation at 673K on 5% Ni/ZrO_2(II), with H_2O in the reactant stream. See Table 3 for description of conditions. Arrows give rate in water-free system.

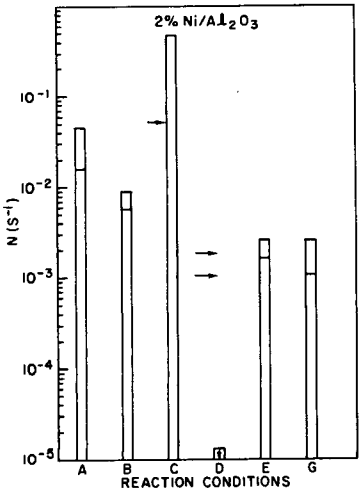

FIG. 5

CO hydrogenation at 673K on 2% Ni/Al_2O_3 with H_2O in the reactant stream. See Table 3 for description of conditions. Arrows give rate in water-free system.

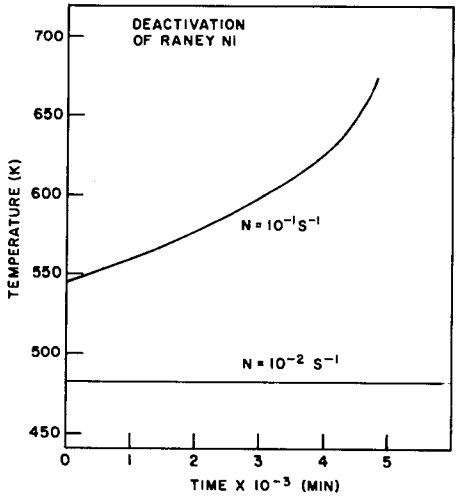

FIG. 6

Deactivation of Raney Ni for CO hydrogenation with reaction time.

FORMATION OF SURFACE CARBON AND METHANATION CATALYSIS ON ALUMINA SUPPORTED NICKEL

by

P. R. Wentrcek, J. G. McCarty, B. J. Wood and H. Wise
Solid State Catalysis Laboratory, Stanford Research Institute
333 Ravenswood Avenue, Menlo Park, California 94025

ABSTRACT

The mechanism of catalytic methanation on an alumina-supported nickel catalyst (25 wt% Ni) has been examined by means of (1) kinetic studies with a pulse microreactor, (2) surface studies with Auger electron spectroscopy (AES), and (3) temperature programmed surface reaction kinetics (TPSR) at the gas/solid interface. During exposure of the catalyst to pulses of CO (diluted with He) at elevated temperatures (> 450 K), we observed first-order formation of surface carbon. The surface carbon so formed exhibited high reactivity towards hydrogen with quantitative conversion to methane. The Auger electron spectra indicated that the surface carbon was bonded to the Ni as a carbidic-type surface species which converted to graphitic carbon of very low reactivity towards hydrogen at temperatures above 675 K. The kinetics of methane formation from surface carbon and gaseous H_2 were determined by means of TPSR. The formation of CH_4 is observed at temperatures as low as 375 K. The rates of methane formation follow first-order kinetics with respect to surface carbon. The activation energy for this process is 17.6 kcal/mol. The experimental data are analyzed in terms of a catalytic methanation mechanism in which dissociative adsorption of carbon monoxide and hydrogen is followed by reaction of surface carbon and surface oxygen with hydrogen adatoms to yield methane and water.

INTRODUCTION

In spite of considerable effort the methanation mechanism on nickel catalysts is not established unequivocally. At room temperature non-dissociative CO adsorption has been reported with the formation of several molecular bonding states on the surface of nickel.[1-5] However at elevated

---

*This research was supported by the American Gas Association.

temperatures (> 350 K) on an alumina-supported Ni catalyst[6] and on Ni films[7] the formation of CO_2 was observed and the reaction interpreted in terms of disproportionation. More recently dissociative chemisorption[8,9] has been suggested in accordance with:

$$CO(g) \rightleftarrows CO(s) \quad (1)$$

$$CO(s) \rightarrow C(s) + O(s) \quad (2)$$

$$CO(g) + O(s) \rightarrow CO_2(g) \quad (3)$$

However the surface carbon so formed was considered to have negligible reactivity in methanation and to deactivate the catalyst with the formation of bulk Ni_3C or graphitic carbon structures.[10]

The objectives of our research were (1) the kinetics of interaction of CO with a Ni/Al_2O_3 catalyst, (2) the reactivity of the surface carbon species toward hydrogen, and (3) the physical nature of the surface carbon and its bonding to Ni by Auger electron spectroscopy.

EXPERIMENTAL DETAILS

For measurement of the reaction of CO with the Ni/Al_2O_3 catalyst a pulse-microreactor system was used operating at 50 psig. Constant-volume pulses (1.3 cm^3) of CO, H_2, or CO/H_2 mixtures (CO + H_2) in a helium carrier stream passed through the catalyst bed and entered a gas chromatograph (GC) for quantitative analysis (CO, CO_2, and CH_4). The catalyst bed consisted of 13.7×10^{-3} g of hydrogen-reduced Girdler G-65 methanation catalyst (25 wt% Ni supported on Al_2O_3) crushed to finer than 200-mesh particle size. The catalyst was reduced for 15 hours at 725 K in a steady stream of pure H_2 at 1 atm, then purged for an hour in flowing He before the temperature was lowered to the desired operating level.

The rates of removal of the surface carbon species by hydrogen were determined by the technique of temperature programmed surface reaction (TPSR). This method represents a modification of the temperature programmed desorption technique (TPD) and is particularly well suited to the study of irreversible surface gas reactions, such as the interaction of hydrogen with surface carbon on nickel.[11] Interpretation of the experimental data in terms of kinetic parameters is based on the same theoretical analysis as employed in TPD.[12]

---

*(s) refers to a surface species and (g) to a gaseous species.

After depositing surface carbon on the catalyst (in the range from 3×10^{14} to 9×10^{14} atoms/cm^2 by exposure to a series of CO/He pulses at 450 - 550 K the sample was cooled to room temperature and the carrier gas changed to hydrogen. Subsequently the catalyst temperature was raised at a linear heating rate and the formation of methane resulting from the reaction of surface carbon with hydrogen was monitored as a function of time and temperature.

EXPERIMENTAL RESULTS

1. Pulse Microreactor Experiments

To establish the reaction order with respect to CO for surface-carbon formation the CO concentration in the pulse contacting the catalyst sample in the microreactor was varied from 1.0 to 10.0 vol% CO (in He) at 553 K. From the amount of CO_2 formed the mass of carbon deposited on the catalyst surface could be calculated (Equations 2 and 3). From the difference between the CO consumed (equivalent to twice the amount of CO_2 formed) and the total CO lost from the pulse the amount of non-dissociated CO left on the catalyst could be determined. The results of a series of such experiments are shown in Figure 1. The data depicted by curve (a) demonstrate that the fractional conversion of CO to surface carbon is proportional to the amount of CO in the pulse, indicative of a first order surface reaction. Thus, rather than disproportionation the mechanism involves rapid CO adsorption and rate-limited dissociation of the CO admolecule (reaction 2), followed by rapid removal of the oxygen adatoms by further reaction with CO [reaction (3)].

Of interest is the quantitative conversion of the surface carbon to methane on exposure to a hydrogen pulse at 553 K (curve b, Figure 1), except at very high surface densities of carbon (an estimated surface coverage of more than 50 percent relative to Ni surface atoms) at which the amount of the carbon converted to methane is somewhat less than that deposited. Under these conditions the temperature-labile characteristics of the surface carbon become apparent, as discussed in further detail in the following section.

For a first-order reaction, such as the dissociative chemisorption of CO on Ni/Al_2O_3, a pulse-reactor experiment can be employed for kinetic studies. Thus, from measurement of the amount of surface carbon formed over a range of temperatures, the activation energy for this heterogeneous reaction can be evaluated.[13] Over a temperature range from 553 K to 613 K we calculate, an activation energy of 39 kcal/mole for reaction (3) on the basis of a heat of adsorption of CO on nickel[7] of -35.0 kcal/mole.

2. TPSR Studies

The rate of formation of CH_4 by interaction of surface carbon with hydrogen, as studied by the TPSR technique, exhibits two distinct maxima (Figure 2). One methane peak is centered at 430 ± 20 K (α state), and the other at 630 ± 20 K (β state). The ratio of carbon coverages between the two states was found to be $N_\alpha/N_\beta = 2.5$ for exposure to CO at 523 K, and $N_\alpha/N_\beta = 1.0$ for exposure at 575 K. The shape of the TPSR curve and the maximum reaction temperatures were not influenced significantly by the temperature of surface-carbon deposition (from 510 to 570 K). In addition, the lack of dependence of these parameters on initial carbon coverage provides strong evidence that the reaction under study is of first order in surface-carbon coverage.

The apparent activation energies for the reaction of hydrogen with both the α and β states of adsorbed carbon were determined by varying the heating rate in a series of TPSR experiments.[12] Based on the theoretical analysis of a first-order surface reaction the apparent activation energies for the reaction of hydrogen with the α- and β- states of surface carbon were calculated:

$$k_\alpha = 1.3 \times 10^7 \exp(-17700/RT) \text{ sec}^{-1} \quad (4)$$

$$k_\beta = 3.0 \times 10^9 \exp(-33000/RT) \text{ sec}^{-1} \quad (5)$$

DISCUSSION

The experimental results strongly suggest the surface carbon formed by dissociative chemisorption of CO as an intermediate in the methanation reaction catalyzed by nickel. This mechanism is reinforced by experimental studies in which the surface carbon deposited to various degrees of surface coverage was exposed to pulses containing either hydrogen or mixtures of H_2 and CO ($H_2/CO = 9/1$). As summarized in Table 1 the surface carbon resulting from the exposure of the Ni/Al_2O_3 catalyst to six consecutive CO pulses can be converted rapidly and quantitatively to methane on exposure to a pulse of hydrogen. The resulting carbon mass balance between methane and surface carbon is excellent. On contacting a catalyst containing surface carbon with a pulse of $H_2/CO(9/1)$ the total amount of methane produced is greatly augmented over that measured on a clean nickel surface with the same gas mixture. As a matter of fact the total number of CH_4 molecules formed approaches the sum of the number of carbon atoms deposited on the catalyst surface and the number of CO molecules converted in passing a CO/H_2 pulse gas mixture over the clean catalyst (Table 1).

Furthermore it should be noted that in pulsing with CO some non-dissociated carbon monoxide is retained by the catalyst (Table 1). However these CO admolecules do not seem to contribute to methane formation on subsequent exposure to a pulse of H_2 at 553 K. This lack of participation of adsorbed CO molecules in methanation is substantiated by a calculation of the site occupancy of carbon and carbon monoxide adspecies on the catalyst surface resulting from exposure to pulses of different CO concentrations. In this analysis the assumption has been made that a bridge-bonded configuration [CO(B)] is particularly favorable for dissociative adsorption of CO, i.e., two neighboring nickel sites onto which CO is bound. The remaining sites are taken to be occupied by linearly bound CO admolecules [CO(L)], i.e., those bonded by sp-hybridized carbon to a single Ni atom. It will be noted from the data in Figure 1 (curve c) that during pulsing with progressively larger doses of CO, the finite number of Ni sites available is quickly preempted by CO(B)so that the adsorption of CO(L) goes through a maximum value. From a comparison of curves b and c in Figure 2 it is apparent that methane formation runs parallel to the surface density of C-atoms and not CO admolecules.

The chemical state of the carbon adatoms on the surface of the Ni/Al_2O_3 catalyst has been determined by means of Auger electron spectroscopic studies. A catalyst sample exposed to several CO pulses (10 vol% in He) at 553 K and cooled to room temperature exhibited the spectrum shown in Figure 3. The Auger electrons with energies near 250 eV and 260 eV exhibited by the Ni/Al_2O_3 sample and the carburized Ni foil are characteristic of a carbidic-type carbon structure.[14,15] The KLL Auger transition near 270 eV is common carbon in both the graphitic and the carbidic chemical states.

Since in the energy range of interest the Auger electrons emanate from a shallow depth near the surface of the solid (< 3 atomic layer) we may conclude that the dissociative chemisorption of CO on Ni results in the formation of a carbidic Ni-C surface bond. From the dissociation energy of CO (256 kcal/mole) and the Ni-O bond strength (89 kcal/mole) we estimate a value of 167 kcal/mole as the lower limit of the Ni-C binding energy required to make dissociative chemisorption of CO on Ni thermodynamically feasible. A bond strength of this magnitude for the Ni-C bond has been reported.[16]

Further evidence for dissociative adsorption of CO on Ni is provided by electron spectroscopy. In a study[17] of the photoelectron spectra of CO adsorbed on a polycrystalline nickel film at 300 K, a density-of-states distribution for the oxygen valence electrons was observed which could be attributed to CO admolecules. However at T > 400 K, the density-of-states distribution changed to that characteristic of O-adatoms resulting

from CO dissociation. Also, for CO adsorption on a disordered Ni(111) surface, Eastman and coworkers[18] reported rupture of the C–O bond.

The labile characteristics of the carbidic surface carbon species on nickel becomes apparent during prolonged exposure of the catalyst surface to the electron beam of the Auger electron spectrometer or to elevated temperatures. Under these conditions the Auger spectrum indicates a gradual transformation of the carbidic carbon to the graphitic form, i.e. disappearance of the spectral fine structure associated with the 250 and 260 eV Auger "peaks" and growth of the signal intensity of the 270 eV "peak." This form of surface carbon is relatively unreactive toward hydrogen. Possibly it has the properties of the C(β)-state (Figure 2) observed in the TPSR experiments. From the rate constants measured we would expect the reactivity of the graphitic carbon towards hydrogen to be 1/10,000 that of the carbidic species at 553 K.

Our experimental work strongly suggests the carbidic carbon surface species as an intermediate in the Ni-catalyzed methanation reaction. This surface carbon species, highly reactive towards hydrogenation and methane formation, should be distinguished from bulk nickel carbide, (Ni_3C), whose activity in methanation catalysis has been examined and found to be relatively low.[19-21] The rate determining step is to be found in the dissociative chemisorption of CO. The activation energy for this process is estimated to be 39 $\pm$ 2 kcal/mole, a value of the same magnitude found in our apparatus for steady state catalytic methanation at CO/H_2 = 1/9, as shown by the data in Figure 4.

REFERENCES

1. R. R. Ford, in Advances in Catalysis, eds. D. D. Eley, H. Pines, and P. B. Weisz, Academic Press, N.Y. 1970, Vol. 21; M. A. Vannice, J. Catalysis, 37, 449 (1975).

2. H. H. Madden, J. Kuppers, and G. Ertl, J. Chem. Phys., 58, 3401 (1973).

3. J. E. Demith and T. N. Rhodin, Surface Sci., 45, 249 (1974).

4. D. A. Degras, Nuovo Cimento Suppl., 5, 408 (1967).

5. G. Wedler, H. Papp, and G. Schroll, Surface Sci., 44, 463 (1974).

6. J. L. Bousquet, P. C. Gravelle, and S. Teichner, Bull. Soc. Chim. Franc., 1972, 3693.

7. M. McD. Baker and E. K. Rideal, Trans. Faraday Soc., 51, 1597 (1955).

8. H. H. Madden and G. Ertl, Surface Sci., 35, 211 (1973).

9. P. B. Tottrup, J. Catalysis 42, 29 (1976).

10. J. R. Rostrup-Nielsen, J. Catalysis 27, 343 (1972).

11. J. G. McCarty and H. Wise (to be published).

12. J. L. Falconer and R. J. Maddix, Surf. Sci. 48, 393 (1975).

13. D. W. Bassett and H. W. Habgood, J. Phys. Chem. 64, 769 (1960).

14. J. P. Coad and J. C. Riviere, Surf. Sci. 25, 609 (1971).

15. T. W. Haas and J. T. Grant. Appl. Phys. Letters 16, 172 (1970); T. W. Haas, J. T. Grant, and G. J. Dooley, J. Appl. Physics 43, 1853 (1972).

16. L. C. Isett and J. M. Blakely, Surf. Sci. 47, 645 (1975).

17. R. W. Joyner and M. W. Roberts, J. Chem. Soc. Faraday Trans. 1, 70, 1819 (1974).

18. D. E. Eastman, J. E. Demith, and J. M. Baker, J. Vac. Sci. Tech., 11, 273 (1974).

19. S. Weller, L.J.E. Hofer, and R. B. Anderson, J. Amer. Chem. Soc., 70, 799 (1948).

20. J. T. Kummer, T. W. DeWitt, and P. H. Emmett, J. Amer. Chem. Soc., 20, 3632 (1948).

21. A. K. Galwey, J. Catalysis 1, 227 (1962).

Table 1

INTERACTION OF H_2 AND H_2/CO WITH SURFACE CARBON ON Ni/Al_2O_3 CATALYST[a] AT 553 K

Experiment	Pulse[b]			Surface Species Deposited (moles x 10^6)		CH_4 Formed (mole x 10^6)
	Composition (vol%)		Total Number			
	H_2	CO		CO	C	
1	0	10	2	1.56	2.01	-
	100	0	1	0	0	1.96
2	0	10	2	0.83	2.12	-
	100	0	1	0	0	2.10
3	0	10	6	1.65	3.40	-
	100	0	1	0	0	3.39
4	90	10	1	-	-	5.25
	0	10	5	-	3.08	-
	90	10	1	-	-	8.01

[a] Ni/Al_2O_3 catalyst (Girdler G-65, 25 wt% Ni).

[b] CO pulse = 5.73×10^{-6} mole; H_2 pulse = 5.73×10^{-5} mole.

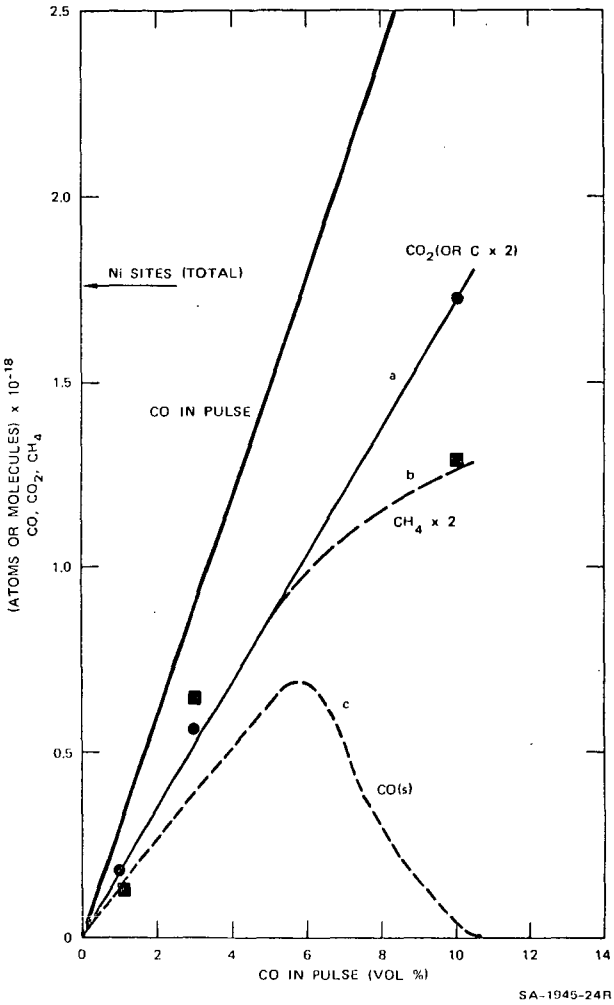

FIGURE 1 SURFACE CARBON INTERMEDIATE IN CATALYTIC METHANATION (Ni/Al_2O_3, 25 wt %)

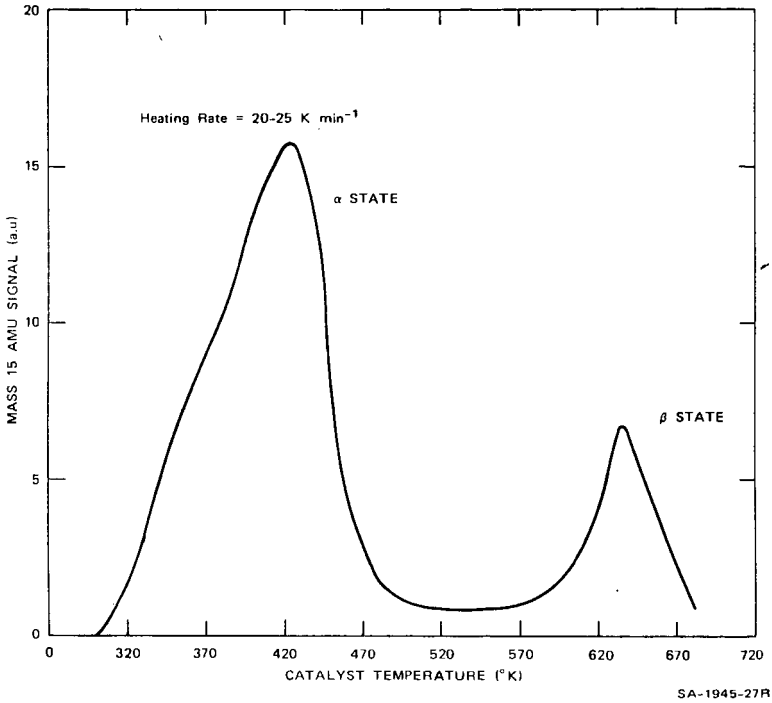

FIGURE 2 TEMPERATURE PROGRAMMED SURFACE REACTION BETWEEN SURFACE CARBON AND GASEOUS HYDROGEN CATALYZED BY Ni/Al_2O_3 (25 wt %)

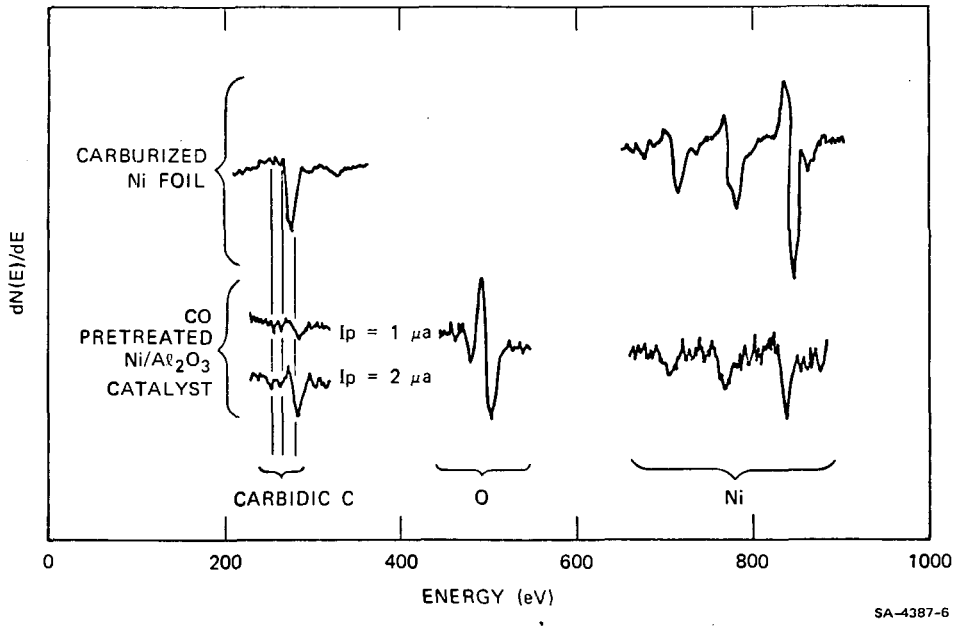

FIGURE 3 AES OF SURFACE CARBON MNi/Al_2O_3 CATALYST AFTER EXPOSURE TO CO AT 553 K

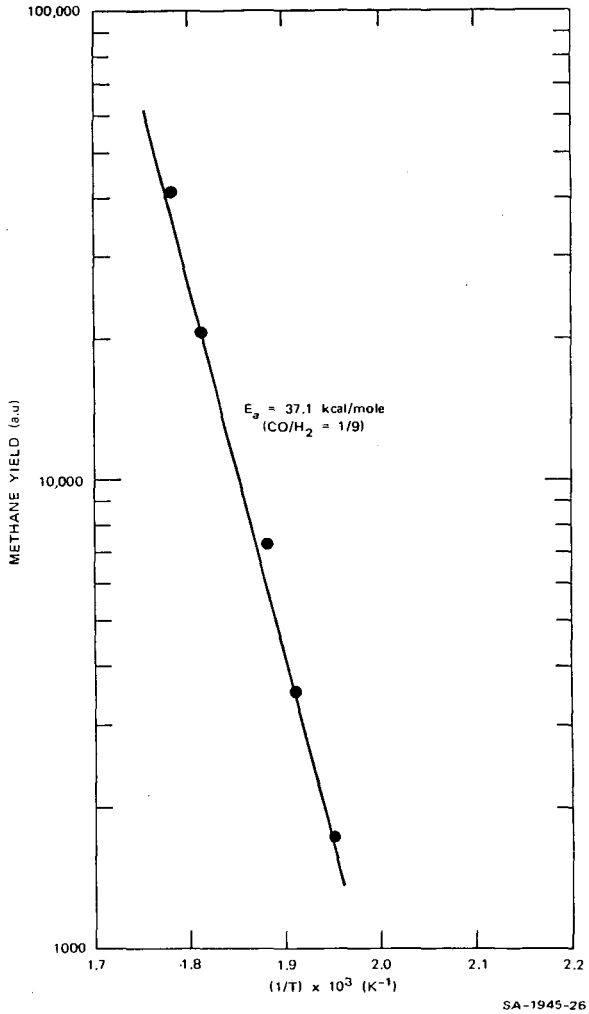

FIGURE 4 STEADY STATE METHANATION ACTIVITY OF Ni/Al_2O_3 (25 wt %)